AFRL-AFOSR-VA-TR-2015-0256

Residual-based Methods for Controlling Discretization Error in CFD

Chris Roy
VIRGINIA POLYTECHNIC INST AND STATE UNIVERSITY

08/24/2015
Final Report

Air Force Research Laboratory
AF Office Of Scientific Research (AFOSR)/ RTA
Arlington, Virginia 22203
Air Force Materiel Command

REPORT DOCUMENTATION PAGE

Form Approved
OMB No. 0704-0188

PLEASE DO NOT RETURN YOUR FORM TO THE ABOVE ORGANIZATION.

1. REPORT DATE *(DD-MM-YYYY)*	2. REPORT TYPE	3. DATES COVERED *(From - To)*
18-08-2015	Final Report	01-05-2012 to 30-04-2015

4. TITLE AND SUBTITLE
Residual-based Methods for Controlling Discretization Error in CFD

5a. CONTRACT NUMBER
FA9550-12-1-0173

5b. GRANT NUMBER

5c. PROGRAM ELEMENT NUMBER

6. AUTHOR(S)
Chris Roy
Aerospace and Ocean Engineering Dept. (MC0203)
Randolph Hall, RM 215, Virginia Tech
460 Old Turner St
Blacksburg, VA 24061
Voice: (540) 231-0080

5d. PROJECT NUMBER

5e. TASK NUMBER

5f. WORK UNIT NUMBER

7. PERFORMING ORGANIZATION NAME(S) AND ADDRESS(ES)
Virginia Tech
300 TURNER ST NW, SUITE 4200
BLACKSBURG, VA 24061

8. PERFORMING ORGANIZATION REPORT NUMBER

9. SPONSORING/MONITORING AGENCY NAME(S) AND ADDRESS(ES)
Air Force Office of Scientific Research
875 N. Randolph Street
Suite 325, Room 3112
Arlington, VA 22203

10. SPONSOR/MONITOR'S ACRONYM(S)
AFOSR

11. SPONSOR/MONITOR'S REPORT NUMBER(S)

12. DISTRIBUTION/AVAILABILITY STATEMENT
Distribution A - Approved for Public Release

13. SUPPLEMENTARY NOTES

14. ABSTRACT

Computational Fluid Dynamics (CFD) has enormous potential to impact the analysis, design, and optimization of U.S. Air Force flight systems. The objective of our work is to develop and demonstrate methods for the reliable and automatic control of discretization error in CFD. Our approach will provide designers and analysts with techniques to quantify and reduce discretization error in CFD predictions without the overhead of creating, and solving on, multiple meshes. Our work will lead to significant improvements in the accuracy and efficiency of CFD predictions of aerodynamic loads. We will investigate the following residual-based discretization error estimation techniques unified within the PI's generalized truncation error estimation framework: discretization error transport equations, defect correction methods, and adjoint methods. We will also develop mesh adaptation techniques wherein the mesh is automatically adapted to reduce discretization error in the solution or solution functionals (i.e., aerodynamic loads). The adaptation will be driven by the residuals/truncation errors, which serve as the local source of discretization error, rather than ad hoc solution features (e.g., gradients, shock waves).

15. SUBJECT TERMS
computational fluid dynamics, simulation uncertainty, error estimation, discretization error

16. SECURITY CLASSIFICATION OF:			17. LIMITATION OF ABSTRACT	18. NUMBER OF PAGES	19a. NAME OF RESPONSIBLE PERSON
a. REPORT	b. ABSTRACT	c. THIS PAGE			Chris Roy
UU	UU	UU	UU	52	19b. TELEPHONE NUMBER *(Include area code)* (540) 231-0080

INSTRUCTIONS FOR COMPLETING SF 298

1. REPORT DATE. Full publication date, including day, month, if available. Must cite at least the year and be Year 2000 compliant, e.g. 30-06-1998; xx-06-1998; xx-xx-1998.

2. REPORT TYPE. State the type of report, such as final, technical, interim, memorandum, master's thesis, progress, quarterly, research, special, group study, etc.

3. DATES COVERED. Indicate the time during which the work was performed and the report was written, e.g., Jun 1997 - Jun 1998; 1-10 Jun 1996; May - Nov 1998; Nov 1998.

4. TITLE. Enter title and subtitle with volume number and part number, if applicable. On classified documents, enter the title classification in parentheses.

5a. CONTRACT NUMBER. Enter all contract numbers as they appear in the report, e.g. F33615-86-C-5169.

5b. GRANT NUMBER. Enter all grant numbers as they appear in the report, e.g. AFOSR-82-1234.

5c. PROGRAM ELEMENT NUMBER. Enter all program element numbers as they appear in the report, e.g. 61101A.

5d. PROJECT NUMBER. Enter all project numbers as they appear in the report, e.g. 1F665702D1257; ILIR.

5e. TASK NUMBER. Enter all task numbers as they appear in the report, e.g. 05; RF0330201; T4112.

5f. WORK UNIT NUMBER. Enter all work unit numbers as they appear in the report, e.g. 001; AFAPL30480105.

6. AUTHOR(S). Enter name(s) of person(s) responsible for writing the report, performing the research, or credited with the content of the report. The form of entry is the last name, first name, middle initial, and additional qualifiers separated by commas, e.g. Smith, Richard, J, Jr.

7. PERFORMING ORGANIZATION NAME(S) AND ADDRESS(ES). Self-explanatory.

8. PERFORMING ORGANIZATION REPORT NUMBER. Enter all unique alphanumeric report numbers assigned by the performing organization, e.g. BRL-1234; AFWL-TR-85-4017-Vol-21-PT-2.

9. SPONSORING/MONITORING AGENCY NAME(S) AND ADDRESS(ES). Enter the name and address of the organization(s) financially responsible for and monitoring the work.

10. SPONSOR/MONITOR'S ACRONYM(S). Enter, if available, e.g. BRL, ARDEC, NADC.

11. SPONSOR/MONITOR'S REPORT NUMBER(S). Enter report number as assigned by the sponsoring/ monitoring agency, if available, e.g. BRL-TR-829; -215.

12. DISTRIBUTION/AVAILABILITY STATEMENT. Use agency-mandated availability statements to indicate the public availability or distribution limitations of the report. If additional limitations/ restrictions or special markings are indicated, follow agency authorization procedures, e.g. RD/FRD, PROPIN, ITAR, etc. Include copyright information.

13. SUPPLEMENTARY NOTES. Enter information not included elsewhere such as: prepared in cooperation with; translation of; report supersedes; old edition number, etc.

14. ABSTRACT. A brief (approximately 200 words) factual summary of the most significant information.

15. SUBJECT TERMS. Key words or phrases identifying major concepts in the report.

16. SECURITY CLASSIFICATION. Enter security classification in accordance with security classification regulations, e.g. U, C, S, etc. If this form contains classified information, stamp classification level on the top and bottom of this page.

17. LIMITATION OF ABSTRACT. This block must be completed to assign a distribution limitation to the abstract. Enter UU (Unclassified Unlimited) or SAR (Same as Report). An entry in this block is necessary if the abstract is to be limited.

Residual-based Methods for Controlling Discretization Error in CFD

PI: Christopher J. Roy, Aerospace and Ocean Engineering Dept., cjroy@vt.edu
Co-I: Jeff Borggaard, Interdisciplinary Center for Applied Mathematics, jborggaard@vt.edu
Virginia Tech, Blacksburg, Virginia

Students Funded under this Grant:
Tyrone Phillips, PhD (2014)
Joseph Derlaga, PhD (2015)

Affiliated Students:
Aniruddha Choudhary, PhD (2014)
Charles Jackson, PhD (expected, 2017)
William Tyson, PhD (expected 2018)

I. Introduction

Computational Fluid Dynamics (CFD) has enormous potential to impact the analysis, design, and optimization of U.S. Air Force systems. However, the predictive capability of CFD depends not only on the validity of the sub-models employed (e.g., turbulence, chemistry, multi-phase flow) and the uncertainties present in the system and surroundings, but also on the ability to reliably estimate and reduce numerical errors (Oberkampf and Roy, 2010; Roy and Oberkampf, 2011). While there are many sources of numerical error in a CFD simulation, the largest and most difficult source to estimate (and that our proposed effort targets) is the error related to the resolution and quality of the spatial mesh, i.e., the spatial discretization error. For example, the recent AIAA Drag Prediction Workshops examined simplified transport aircraft challenge cases computed by numerous CFD practitioners; however, even after three such workshops, analysis of the results found that "grids remain a first order effect" (Morrison and Hemsch, 2007). While this proposal is focused on the reliable estimation and control of discretization error in CFD, the proposed techniques also apply to other areas such as computational structural mechanics, computational heat transfer, etc.

Most compressible CFD codes employ finite volume or finite difference discretizations. While there has been a great deal of work on discretization error estimation for finite element method (mainly for elliptic problems), compressible CFD codes tend to rely on simple approaches such as Richardson extrapolation. The main drawback to Richardson extrapolation is that it requires two, or even three, systematically-refined grids in order to obtain the error estimate. For most practical applications, each grid cell is usually refined by a factor of two for each spatial direction, resulting in eight new fine grid cells being generated for each coarse grid cell. For 3D applications, if the coarse grid uses 10 million cells, then two additional levels of refinement would involve 80 million and 640 million cells. Such large cell counts are prohibitively expensive, especially when the original coarse grid provides adequate solutions and the additional grid levels are simply required for the error estimates. Reliable discretization error estimates are needed both for the estimation of total predictive uncertainty in a simulation and to provide a stopping criteria for mesh adaptation strategies.

Automatic mesh adaptation for CFD has been a goal of researchers for more than three decades. However, an examination of current government and industry CFD codes shows that the dream of robust and automatic mesh adaptation has not yet been realized. The few CFD codes that do claim to do mesh

adaptation usually drive it with simple criteria such as solution gradients or curvature (i.e., Hessians); however, these approaches can fail disastrously for complex problems (Ainsworth and Oden, 2000; Dwight, 2008). Mathematically rigorous approaches for driving mesh adaptation are discussed in this proposal. Once the strategy for driving the adaption is chosen, a technique must be chosen for actually accomplishing the adaptation. Adaptation approaches for compressible CFD computations are practically limited to mesh movement (i.e., r-adaptation) for structured grids and r- and h- adaptation (i.e., local cell additions/deletions) for unstructured grids. Adaptation based on changing the local formal order of accuracy of the scheme (i.e., p-adaptation) for compressible CFD codes (especially on unstructured grids) is difficult, although some progress is being made through the use of discontinuous Galerkin methods (Hesthaven and Warburton, 2008). Automatic mesh adaptation is required for complex CFD problems in order to obtain reliable discretization error estimates.

Inaccurate prediction of aerodynamic loads was found to be the leading cause of unanticipated structural response or damage (Love et al., 2003), costing the U.S. Air Force billions of dollars and adversely impacting system readiness. Our approach will provide designers and analysts with techniques to quantify and reduce discretization error in CFD predictions without the overhead of creating, and solving on, multiple meshes. Our work will lead to significant improvements in the accuracy and efficiency of CFD predictions of aerodynamic loads. The outcomes of the proposed work will be improved aerodynamic predictions for preliminary design, parametric studies, sensitivity analysis, uncertainty quantification, optimization, optimization under uncertainty, and multiphysics computations.

II. Background

The discretization error is the numerical error due to the mesh and time step chosen for the simulation. It is formally defined as the difference between the exact solution to the discrete equations and the exact solution to the underlying partial differential or integral equations (referred to collectively as the PDEs in this proposal). This relationship is given in equation form as

$$\varepsilon_h = u_h - \tilde{u} \tag{1}$$

where ε_h is the local discretization error, u_h is the numerical solution (neglecting iterative and round-off error), and $\tilde{u}$ denotes the exact solution to the PDEs.

Truncation Error Framework

The truncation error is the difference between the discrete equation and the underlying PDE and can be found by using Taylor series expansions. A simple example of a truncation error analysis follows. Consider 1D steady Burgers' equation

$$u\frac{du}{dx} - \nu\frac{d^2u}{dx^2} = 0 \tag{2}$$

which provides a simple, scalar, nonlinear model equation for the Navier-Stokes equations as it contains nonlinear convection and linear diffusion with constant viscosity ν. Burgers' equation will be used as a simple example throughout this proposal. For a simple second-order accurate finite difference discretization of Burgers' equation using a constant mesh spacing $h = \Delta x$, a truncation error analysis gives

$$\underbrace{u_i\left(\frac{u_{i+1}-u_{i-1}}{2\Delta x}\right)-\nu\left(\frac{u_{i+1}-2u_i+u_{i-1}}{\Delta x^2}\right)}_{L_h(u)}=\underbrace{u_i\left.\frac{du}{dx}\right|_i-\nu\left.\frac{d^2u}{dx^2}\right|_i}_{L(u)}+\underbrace{u_i\left.\frac{d^3u}{dx^3}\right|_i\frac{\Delta x^2}{6}-\nu\left.\frac{d^4u}{dx^4}\right|_i\frac{\Delta x^2}{12}+O\left[\Delta x^4\right]}_{\tau_h(u)}$$

where $L_h(u)$ is the discrete operator, $L(u)$ the PDE operator (here it is restricted to the nodes), and $\tau_h(u)$ is the truncation error. The discrete equations are exactly satisfied by the discrete solution at the nodes u_h (i.e., $L_h(u_h)=0$), the PDE is exactly solved by its continuous solution (i.e., $L(\tilde{u})=0$), and the truncation error operates on a continuous function but produces discrete values. This is a general relationship for arbitrary (but smooth) $u(x)$ which assumes appropriate operators are used to restrict continuous functions to discrete points or prolong discrete functions to a continuous space (see the Technical Approach section for a more rigorous discussion). Using the above operator notation, this relationship can be expressed as the *Generalized Truncation Error Expression* (GTEE) (Roy, 2009 and 2010a):

$$L_h(u)=L(u)+\tau_h(u)\,. \tag{3}$$

The relationship between the truncation error and the discretization error can be established by examining the continuous discretization error transport equation. Inserting the exact solution to the discrete equations u_h into Equation (3), then subtracting the original (continuous) governing equation $L(\tilde{u})=0$ gives

$$L(u_h)-L(\tilde{u})+\tau_h(u_h)=0\,.$$

If the operator is linear (or has been linearized by assuming $\tilde{u}\approx u_h$), then $L(u_h)-L(\tilde{u})=L(u_h-\tilde{u})$. Employing the definition of the discretization error from Equation (1) results in

$$L(\varepsilon_h)=-\tau_h(u_h) \tag{4}$$

which for Burgers' equation becomes

$$u\frac{d\varepsilon_h}{dx}-\nu\frac{d^2\varepsilon_h}{dx^2}=-u\frac{d^3u_h}{dx^3}\frac{\Delta x^2}{6}+\nu\frac{d^4u_h}{dx^4}\frac{\Delta x^2}{12}+O\left[\Delta x^4\right]. \tag{5}$$

Equations (4) and (5) represent a continuous transport equation (similar to the error equation in finite elements) which can be solved on the same grid as the original problem to estimate the discretization error. It shows that discretization error is transported in the same manner as the solution, and that it is locally generated by the truncation error. When the truncation error is reduced, then the local source for the discretization error is also reduced, leading to less discretization error "production" over the domain. Broadly speaking, when globally "good" numerical solutions are desired, then the truncation error is the ideal driver for mesh adaptation (Baker, 1997; Roy, 2009). When only a small number of solution functionals are of interest (e.g., lift or drag in an aerodynamics simulation), then adjoint methods can be used to account for the sensitivity of the solution functional to local truncation errors (e.g., Pierce and Giles, 2000; Venditti and Darmofal, 2003).

Discretization Error Estimators

The discretization error ε_h was given in Equation (1) and is formally defined as the difference between the exact solution to the discrete equations u_h and the exact solution to the underlying PDEs $\tilde{u}$. The spatial discretization error is generally the largest contributor to the overall numerical error, with the other contributors being temporal discretization error, iterative convergence error, and round-off error. There are two types of discretization error estimators (Roy, 2010a). The first involves comparing the numerical solution (or its gradients) to higher-order accurate estimates of the solution (gradients). Included in this category are Richardson extrapolation for the solution and solution functionals which requires solutions on multiple meshes (Roy, 2005) and recovery-based methods for gradients from finite elements (e.g., Zienkiewicz and Zhu, 1992). The second class of methods for estimating discretization error employs either the continuous or discrete residual (not to be confused with the iterative residuals which are often used to monitor iterative convergence) or, equivalently, the truncation error. Residual-based methods employ information about the problem being solved and include error transport equations (e.g., Cavallo and Sinha, 2007), defect correction (e.g., Skeel, 1986), adjoint methods (e.g., Venditti and Darmofal, 2003), and explicit/implicit residual methods from finite elements (Ainsworth and Oden, 2000). Finally, there is a hybrid approach called least squares extrapolation where the extrapolation employs unknown, spatially varying coefficients which are determined by minimizing the residual on a finer mesh (Garbey and Shyy, 2003).

Spatial discretization error is the most difficult type of numerical error to estimate reliably. Regardless of the approach used to estimate the discretization error, the numerical solution(s) must be in the asymptotic range in order to obtain reliable estimates. The asymptotic range is defined as the range of mesh resolutions where the discretization error reduces at the theoretical (i.e., formal) rate with mesh refinement. This asymptotic range is defined only in terms of systematic mesh refinement (Oberkampf and Roy, 2010) where the mesh is refined uniformly by a factor h in each coordinate direction, e.g.,

$$h = \frac{\Delta x}{\Delta x_{ref}} = \frac{\Delta y}{\Delta y_{ref}} = \frac{\Delta z}{\Delta z_{ref}} \tag{6}$$

and the mesh quality is constant or improves with mesh refinement. Ensuring systematic mesh refinement can be challenging, especially for unstructured meshes which contain more than one type of mesh topology (e.g., hexahedral, tetrahedral, and prismatic elements).

Verifying that the solutions are in the asymptotic range is traditionally done by computing the observed order of accuracy using numerical solutions on three systematically-refined meshes. For systematic refinement by the factor r, one has $h_{fine} = h$, $h_{medium} = rh$, and $h_{coarse} = r^2h$ and the observed order of accuracy $\hat{p}$ can be found as (Roache, 2009):

$$\hat{p} = \frac{\ln\left(\dfrac{f_{r^2h} - f_{rh}}{f_{rh} - f_h}\right)}{\ln(r)}. \tag{7}$$

The grid refinement factor can generally be as small $r = 1.1$ without round-off and iterative error polluting the results; however, from a practical standpoint, a refinement factor of $r = 2$ is often used which implies insertion of new nodes between each existing node for structured grids and local sub-division of elements in unstructured grids. For three-dimensional flows, $r = 2$ results in a factor of 8 increase in total grid cells for each level of refinement and can thus be prohibitively expensive. Furthermore, the observed order of

accuracy will only match the formal order when all three grid levels are in the asymptotic range. A major challenge is to obtain reliable discretization error estimates without requiring solutions with hundreds of millions of cells. For practical problems, it is our opinion that the asymptotic range is not achievable (or at least demonstrable) without effective local mesh adaptation strategies.

Truncation Error and Residuals

The truncation error can be related to the residuals used in residual-based error estimators and adjoint methods. Inserting the numerical solution u_h into the GTEE given in Equation (3) gives the continuous residual

$$L(u_h) = -\tau_h(u_h) \tag{8}$$

which is analogous to the finite element residual (Ainsworth and Oden, 2000) and the source term used in the differential form of defect correction (Skeel, 1986). If instead the exact solution to the continuous governing equation $\tilde{u}$ (or an approximation thereof) is inserted into the GTEE, one obtains the discrete residual

$$L_h(\tilde{u}) = \tau_h(\tilde{u}) . \tag{9}$$

It is this discrete residual (or its approximation) that is approximated in many adjoint methods (Venditti and Darmofal, 2003) and discretization error transport equations (e.g., Shih and Williams, 2009).

Mesh Adaptation

There are two main approaches for performing mesh adaption. Mesh refinement (h-adaptation) provides for the sub-division of mesh cells to improve mesh resolution, while mesh movement (r-adaptation) seeks to move mesh cells from one region to another. For general unstructured grid methods the h-adaption approach is the most popular, while for structured grid methods the r-adaption approach is most often used. In both h- and r-adaptation, weighting functions are generally employed to drive the adaptation process. Regardless of how the adaptation is performed, the more difficult challenge is finding an appropriate criterion to adapt on. The mesh adaptation criterion that is found in most commercial CFD codes is based on solution features such as solution gradients, solution curvature, vortex cores, or shock waves. However, feature-based adaptation is certainly not optimal (Roy, 2009) and can even fail to reduce the discretization error in some cases (e.g., Ainsworth and Oden, 2000; Dwight, 2008).

Since it is the discretization error that one would like to reduce, at first glance, it might appear that the discretization error would be a good criterion to drive the adaptation process. However adaptation based on the discretization error is prone to adapting to components of the discretization error that have been transported from other regions of the domain rather than the error that is locally generated (Gu and Shih, 2001; Roy, 2009). The successful use of recovery-based mesh adaptation in finite elements, where adaptation is driven by the estimated discretization error in the solution gradients, relies on the superconvergence property of finite element methods (Ainsworth and Oden, 2000), as well as possibly the elliptic mathematical character of the equations. A recovery-type method for finite volume schemes has also been developed based on the solution interpolation error (e.g., see McRae 2000). Recovery-based methods are not appropriate for driving mesh adaptation in cases where the governing equations are hyperbolic or when finite difference or finite volume methods are used.

Examination of the continuous discretization error transport equation (called the error equation in finite elements) given by Equation (4) shows that underlying PDE transports the discretization error in the same fashion as the solution properties. For our Burgers' equation example, the error transport equation given by Equation (5) shows that the error will be both convected at the local velocity and locally diffused according to the viscosity. More importantly, it shows that the truncation error serves as a local source term for the discretization error; thus it is the truncation error (or its approximation) that should be used to drive the mesh adaptation process. The simplest approach is to use the magnitude of the local truncation error to drive the adaptation process. A more advanced approach is to account for both the mesh resolution components and the mesh quality components (stretching, skewness, aspect ratio, etc.) when adapting (Yamaleev, 2001; Alyanak et al., 2011). Finally, if one is interested in only a small number of solution functionals (e.g., lift and drag), adjoint methods can be used to drive adaption by including sensitivities of those functionals to the local truncation error (e.g., Venditti and Darmofal, 2003; Wang and Mavriplis, 2009; Fidkowski and Darmofal, 2011).

III. Objective

The overall objective of our effort was to develop and demonstrate robust, reliable, and automatic methods for controlling discretization error for CFD applications. These methods are based on rigorous theory rather than *ad hoc* approaches such as feature-based adaptation. Given the ambitious nature of this objective, we limit the scope of the problem by restricting our applications to steady-state CFD problems on structured grids; however, we specifically targeted approaches which are extendible to unstructured grids. The focus is on practical CFD applications, with the ultimate application being the steady 3D Reynolds-Averaged Navier-Stokes (RANS) equations. The RANS equations are chosen for their applicability to design, analysis, and optimization of aerospace flight and propulsion systems. The proposed approaches are applicable to all discretization methods (finite difference, finite volume, and finite element) and ultimately extendable across the entire Mach number range including subsonic, transonic, supersonic, and hypersonic speeds.

IV. CFD Code

The CFD code that served as the basis for this work is the finite volume Euler/Navier-Stokes solver developed by our group (Derlaga et al., 2013). The code employs structured grids and has options for various explicit and implicit iterative schemes. Several code enhancements were made during this effort including extension to laminar Navier-Stokes, 3D, and parallelism. All coding implementations were done in a modular fashion to allow future code development.

V. Technical Approach

Our work can be grouped into four broad tasks. Our initial efforts focused on methods for estimating the truncation error. The second task addressed the further development and refinement of the GTEE framework including the required properties of the interpolation operators to be used. The third task involved the development and evaluation of residual-based discretization error estimators within the GTEE framework and includes error transport equation, defect correction, and adjoint methods. The final task was to develop and evaluate mesh adaptation strategies that are based on the residual/truncation error.

VI. Truncation Error Estimation

Framework for Residual-Based Discretization Error Estimation

As discussed earlier, the original Generalized Truncation Error Expression (GTEE) requires appropriate operators to prolong discrete quantities (e.g., finite volume solutions at cell centers) to continuous functions and to restrict continuous functions to cell center or nodal locations (Roy, 2009). We introduce the interpolation function I which can perform both prolongation and restriction operations. This interpolation function is designed to be read from bottom to top. Consider the following examples where u_h is a discrete numerical solution on a fine mesh, u_{2h} is a discrete numerical solution on a coarse mesh, and $\tilde{u}$ is the continuous exact solution to the governing PDEs:

- prolongation of u_h to a continuous space: $I_h u_h$
- prolongation of u_{2h} to mesh *h:* $I_{2h}^h u_{2h}$
- restriction of u_h to mesh *2h:* $I_h^{2h} u_h$
- restriction of $\tilde{u}$ to mesh *h*: $I^h \tilde{u}$

When no subscript or superscript is present, a continuous function is assumed. Using this interpolation operator, the GTEE can be rigorously recast for finite difference and finite volume schemes as

$$L_h(I^h \tilde{w}) = I^h L(\tilde{w}) + \tau_h(\tilde{w}) \tag{10}$$

for any general smooth function $\tilde{w}$. The three terms in Equation (10) refer to nodal values for finite difference methods and cell-averaged values for finite volume methods. In addition, the discretization error definition from Equation (1) can be formulated either continuously or discretely as

$$\varepsilon = I_h u_h - \tilde{u} \qquad \text{or} \qquad \varepsilon_h = u_h - I^h \tilde{u}\,, \tag{11}$$

respectively.

If we consider a discretized function, then the GTEE can be written as

$$L_h(w_h) = I^h L(I_h w_h) + \tau_h(I_h w_h)\,. \tag{12}$$

The prolongation from discrete space to continuous space is an approximation that is better written as

$$I_h = I_h^q + O(h^{q+1}) \tag{13}$$

to account for the error in the prolongation, where q is the order of the reconstructed polynomial for which the k-exact and ENO schemes are q+1 order accurate. Equation (12) is then written as

$$L_h(w_h) = I^h L(I_h^q w_h + O(h^{q+1})) + \tau_h(I_h^q w_h) + O(h^{q+1})\,. \tag{14}$$

or

$$L_h(w_h) = I^h L(I_h^q w_h) + \tau_h(I_h^q w_h) + O(h^{\bar{q}}) . \tag{15}$$

where $\bar{q}$ is an order of accuracy which is related to q but may be modified by nonlinearities in the $L(\cdot)$ and $\tau_h(\cdot)$ operators. Due to the error in the prolongation, it cannot be generally assumed that $w_h = I^h I_h w_h$ unless finite volume consistent reconstructions/prolongations are used, i.e., reconstructions that will exactly integrate out to the average value over the cell.

As is evident from the GTEE, the truncation error is the difference between the discrete and continuous governing equations and has been shown to be the local source of discretization error in a numerical solution (Roy, 2009) where the discrete form of the discretization error is defined as the right side of Equation (11). Here, u_h is the exact solution to the discrete equations such that $L_h(u_h) = 0$, and $\tilde{u}$ is the exact solution to the original governing equations such that $L(\tilde{u}) = 0$. The accurate estimation of truncation error is a key aspect to several residual-based discretization error estimation methods such as the error transport equations (Zhang et al., 2002; Qin and Shih, 2002), defect correction (Pereyra, 1965; Stetter, 1978; Skeel, 1986), and adjoint methods (Giles and Pierce, 2000). Also, as the local source of discretization error, truncation error has been shown to be an effective mesh adaption indicator (Roy, 2009), possibly with adjoint weighting (Venditti and Darmofal, 2003).

The focus of this report is a truncation error estimation method which requires a prolongation of the numerical solution to a continuous space. Inserting the exact solution to the discrete equations u_h into Equation (15), and noting that $L_h(u_h) = 0$, results in

$$\tau_h(I_h^q u_h) = -I^h L(I_h^q u_h) + O(h^{\bar{q}}) . \tag{16}$$

The accuracy of the truncation error estimate is determined by comparing the estimated truncation error to the exact truncation error which requires the exact solution to the governing equations. It can be found by inserting the exact solution into the GTEE and, noting that $L(\tilde{u}) = 0$, gives

$$\tau_h(\tilde{u}) = L_h(I^h \tilde{u}) \tag{17}$$

where the exact and approximate truncation errors are related by

$$\tau_h(\tilde{u}) = \tau_h(I_h u_h) \approx \tau_h(I_h^q u_h) . \tag{18}$$

Various method of estimating truncation error have been developed and tend to be specific to the application. For example, adjoint methods typically use an embedded grid approach developed by Venditti and Darmofal (2003). This method inserts a coarse grid solution into a finer grid using a reconstruction method

$$\tau_h(I_h u_h) = -I_{h/r}^h L_{h/r}(I_q^{h/r} I_h^q u_h) + O(h^{\bar{q}}) . \tag{19}$$

where h represents the coarse grid and h/r represents the fine grid (refined by factor r). We modified this method (Phillips and Roy, 2011) to improve accuracy since the truncation error on the fine grid solution is still significant for second-order schemes with typical refinement factors of two. Equation (19) is

modified to include the effects the fine grid truncation error assuming that the truncation error is asymptotic so that $\tau_h = \frac{\tau_{h/r}}{r^{p_f}}$ where p_f is the formal order of accuracy of the truncation error:

$$\tau_h(I_h u_h) = -I^h_{h/r} L_{h/r}(I^{h/r}_q I^q_h u_h)\left(\frac{r^{p_f}}{r^{p_f}-1}\right) + O(h^{\bar{q}}) . \tag{20}$$

A detailed derivation is given in by Phillips and Roy (2011). The formal order of truncation error is related to the formal order of accuracy of the discretization error; however, for unstructured grids or grids with non-smooth transformations (e.g., with randomly perturbed nodes), the formal order of truncation error can be lower than the formal order of the discretization error (Diskin and Thomas, 2007). Shih and Williams (2009) estimated truncation error for the error transport equations by inserting a finer grid solution into the coarse grid discrete operator

$$\tau_h(I_h u_h) = L_h(I^h_{h/r} u_{h/r}) . \tag{21}$$

Fulton (2003) used a similar embedded grid approach for finite difference discretization schemes, but adjusted the truncation error estimate to take into account the relative magnitudes of the truncation error between the two grids

$$\tau_h(I_h u_h) = L_h(I^h_{h/r} u_{h/r})\left(\frac{r^{p_f}}{r^{p_f}-1}\right). \tag{22}$$

Fraysse et al. (2012) extended Fulton's work to finite volume methods and included the effects of iterative convergence error for numerical solutions which are not fully converged. Under this research grant, we followed a similar approach but re-interpolated the estimated truncation error back onto the computational grid

$$\tau_h(I_h u_h) = I^h_q I^q_{rh} L_{rh}(I^{rh}_h u_h)\left(\frac{1}{r^{p_f}-1}\right) + O(h^{q+1}) . \tag{23}$$

A detailed derivation is given in by Phillips and Roy (2011).

Solution Reconstruction

The cell average of the reconstructed solution is computed using a Curtis-Clenshaw (Clenshaw and Curtis, 1960) quadrature which is extended to multiple dimensions using Smolyak's (Smolyak, 1963) sparse grid construction. We chose Curtis-Clenshaw over the more common Gauss quadrature because the integration points are nested (i.e., higher-order reconstructions use all of the lower order quadrature points) thus allowing adaptive reconstruction and inexpensive quadrature error estimates. The Curtis-Clenshaw quadrature exactly integrates a q-th order polynomial using q+1 function evaluations in one dimension. The quadrature domain $\vec{\xi}$ is a hypercube over the range $0 \le \vec{\xi} \le 1$ so for integration of arbitrary cells a 1st-order polynomial is used to map the arbitrary cell to the quadrature domain where the highest polynomial order for each dimension is one. For example, in two dimensions the polynomial takes the form

$$x_1(\vec{\xi}) = a_{x1} + b_{x1}\xi_1 + c_{x1}\xi_2 + d_{x1}\xi_1\xi_2 . \tag{24}$$

This polynomial is used to exactly constrain the transformation. Given the Curtis-Clenshaw function evaluation points $\vec{\xi}_{cc}$ and weights $\vec{w}$, the integral of a function over an arbitrarily dimensioned hypercube is

$$\frac{1}{V_i}\int_{V_i} f(\vec{x})\,dV = \frac{1}{V_i}\sum_{j=1}^{N_{cc}} f\left(\vec{x}(\vec{\xi}_{j,cc})\right) w_{j,cc}\left|\det\left(J(\vec{\xi}_{j,cc})\right)\right| . \tag{25}$$

where J is the Jacobian of the coordinate transformation and the weights can be found from Burkardt (2010). Because of the non-linear term in the transformation, the Jacobian is not necessarily constant.

The linear system for solution reconstruction is assembled from a stencil of N_{st} cells. To mitigate the effects of round-off error and prevent ill-conditioned systems, the reconstruction is computed on the domain $\xi_{fit} = [0, 1]$ and requires an additional linear transformation to go from the fit domain to the Curtis-Clenshaw domain

$$\xi_{fit}^{(n)} = \frac{\xi_{cc}}{N_{st}} + \frac{n-1}{N_{st}} . \tag{26}$$

where n is the cell number in the reconstruction stencil.

Equation (25) is written more appropriately using matrix notation as

$$V_i u_{i,h} = \vec{w}_{cc}^{T} P\left(\vec{\xi}_{fit}^{(n)}(\xi_{cc})\right)\vec{C} . \tag{27}$$

where for the i-th cell in the reconstruction stencil, $\vec{w}$ is a column vector of weights returned from the Curtis-Clenshaw quadrature, $P(\vec{x}_i)$ is the coefficient matrix for a polynomial fit of size $Ncc \times (k+1)^d$, and $\vec{C}$ is a column vector of the unknown polynomial coefficients.

The complete linear system is written as

$$\vec{W}C = \vec{V}^{T}\vec{u}_h . \tag{28}$$

where $\vec{V}$ is a column vector of cell volumes and for the n-th row $\vec{W}_n = \vec{w}_{cc}^{T} P\left(\vec{x}_n(\vec{\xi}_{cc})\right)$. If the stencil does not change, then this equation can be solved prior to computing the reconstruction for computational efficiency. For all solution reconstructions in this work, polynomial orders from one to four are considered.

k-Exact Method

The k-exact method developed by Barth (1990, 1993) was designed to conserve the mean value of the cell, reconstruct polynomials of degree k or less exactly, be compact, and be computationally efficient. For a polynomial of order k there are k+1 unknowns and $N_{st} = k$+1. For higher dimensions, the polynomial is a tensor product of one-dimensional polynomials with $(k+1)^d$ unknowns where d is the dimension and $N_{st} = (k+1)^d$. A centered stencil is used for the interior of the domain and a shifted stencil near the computational boundary. The reconstruction guarantees that the average value over each cell used in the reconstruction reproduces the numerical solution

$$u_h = I_k^h I_h^k u_h \,. \tag{29}$$

The k-exact method is solved in a least squares sense by increasing the size of the stencil so that Equation 3.25 is valid only for the cell of interest. The method implemented here results in the smallest possible stencil and is equally sized in each coordinate dimension. The conservation of the mean is important in the context of truncation error estimation so that

$$L_h(I_k^h I_h^k u_h) = 0 \,. \tag{30}$$

ENO Method

The ENO method developed by Harten (1987) was extended to arbitrarily dimensions by Godfrey et al. (1993). The reconstruction-via-primitive ENO (RP-ENO) can achieve arbitrary high order accuracy, but is computationally expensive. Godfrey et al. (1993) also introduced a less computationally expensive dimensionally split ENO (DS-ENO) method but does not include cross-derivative terms. The basis of the ENO method is the selection of the stencil to reduce the variation of the solution used to compute the reconstruction. Starting at cell i, the difference between the solutions to the left (i - 1) and right (i + 1) are compared and the minimum is added to the reconstruction stencil. The divided difference is repeated until the stencil has N_{st} points.

RP-ENO Method

The RP-ENO scheme computes the left and right states of a cell using progressive one dimensional curve-fits with the adaptive stencils. For a two-dimensional reconstruction the line-averaged solution in the η-direction is first computed from a one dimensional solution reconstruction where the stencil extends in the ξ-direction

$$p_i(\xi) = \frac{1}{\Delta\eta} \int_{j-1/2}^{j+1/2} u_{i,h}(\xi,\eta) d\eta \,. \tag{31}$$

The reconstructed solution is evaluated at the cell boundaries $p_i([\xi_{i-1/2}^+, \xi_{i+1/2}^-])$ for all cells in the domain. Next, the solution is reconstructed at the left and right faces using a one dimensional reconstruction of the left and right face line averaged values with a stencil that extends in the η-direction. The reconstructed solution is then used to compute the flux at the left and right cell faces. The process is repeated for the top and bottom faces of the cell by computing the line averaged solution in the ξ-direction first. A similar process is followed for three dimensional reconstructions.

DS-ENO Method

The dimensionally split ENO scheme follows the same procedure except only one reconstruction is computed for each face to compute the line-averaged solution in the η-direction and the left and right faces and the line-averaged solution in the ξ-direction at the top and bottom faces. The average solution is used to compute the flux instead of the reconstructed local solution which does not capture the cross-derivative terms. The computational cost of the DS-ENO method is an order of magnitude cheaper than the RP-ENO and k-exact reconstruction methods; however, in our case, computational expense is less of a concern since the truncation error is generally a one-time estimate.

Truncation Error Estimation Results

Burgers' Equation

Burgers' equation is a useful scalar example problem to illustrate and initially test solution reconstruction methods. Burgers' equation is chosen because it is analogous to the Navier-Stokes equations including a non-linear convective term and a linear diffusive term. The conservative form of Burgers' equation is

$$\frac{\partial u}{\partial t} + \int_S \left(\frac{u^2}{2} - \nu \frac{\partial u}{\partial x} \right) dS \,. \tag{32}$$

An exact solution for a viscous shock is

$$\tilde{u}(x) = -u_{ref} \tanh\left(\frac{\mathrm{Re}}{2L} x \right). \tag{33}$$

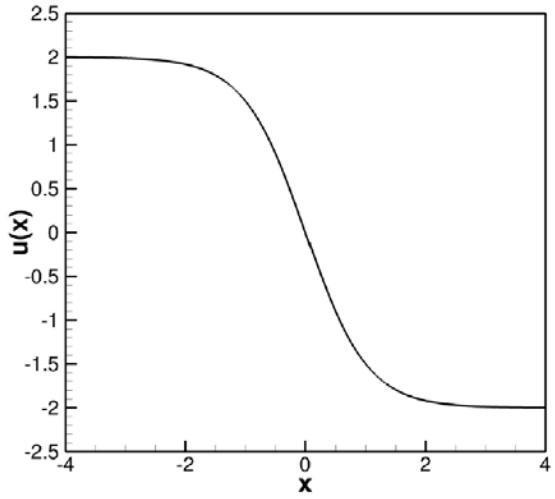

Figure 1. Burgers' Equation exact solution for Re = 16 and 513 grid nodes.

where Re is the Reynolds number, L is a reference length (here $L = 8$), and u_{ref} is chosen as two. The exact solution with Re = 16 is shown in Figure 1. This equation is solved using an explicit, cell-centered finite volume scheme where

$$\frac{u_i^{n+1} - u_i^{n+1}}{\Delta t} + \frac{F_{i+1/2}^n - F_{i-1/2}^n}{\Delta x} = 0 \,. \tag{34}$$

and

$$F_{i+1/2}^n = \frac{u_{i+1}^2 + u_i^2}{2} - \nu \frac{u_{i+1} - u_i}{\left(\Delta x_{i+1} + \Delta x_i \right)/2} \,. \tag{35}$$

Green's theorem is used to compute the gradient ∂u/∂x in Equation (35) which is equivalent to a finite difference on a Cartesian grid.

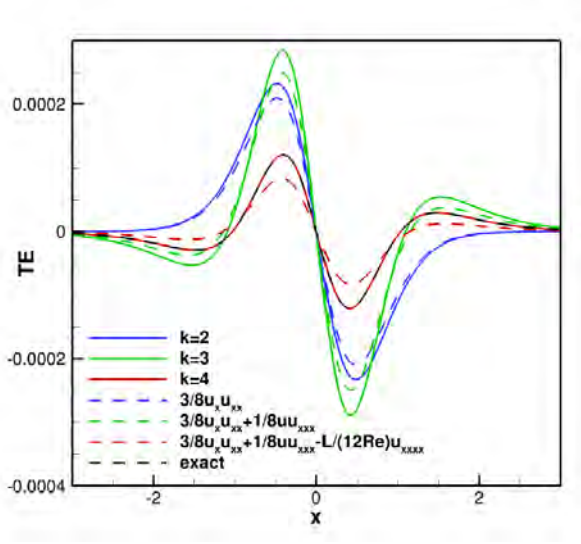

Figure 2. Burgers' Equation truncation error estimate for Re = 16 and 513 grid nodes.

The full truncation error expression consists of an infinite series and can only be exactly calculated using Equation (17) which requires the exact solution; however, for sufficiently fine grids, only the leading truncation error terms need to be accurately estimated. In general, the leading terms are not derived because of the complexity of discretization schemes, but Burgers' equation is simple enough that this is relatively easy. On a grid with equal spacing the leading truncation error terms are

$$\tau_h(u) = \Delta x^2\left(\frac{3}{8}u_x u_{xx} + \frac{1}{8}uu_{xxx} - \frac{1}{24}\nu u_{xxxx}\right) + O(\Delta x^4)\,. \tag{36}$$

From Equation (33) it is clear that this is a second-order accurate scheme and that the next highest truncation error terms are fourth-order accurate. For an accurate estimate of the leading terms the error between the estimated truncation error and the exact truncation should decrease at at least a fourth-order rate.

The discrete solution with Re = 16 computed using 513 grid nodes is reconstructed using the k-exact reconstruction method with k = 2, 3, and 4. The minimum value for k is two because the highest derivative in the governing equations is two and any value of k less than this would result in a derivative term reducing to zero. The truncation error is estimated from the solution reconstructions using Equation (16) and the results are shown in Figure 2. The estimated truncation error is compared to the exact truncation error computed using Equation (17). The estimated truncation error for k = 4 is indistinguishable from the exact truncation error and the error between the exact and estimated truncation error decreases at a fourth-order rate. The other two reconstruction methods, k = 2 and 3, do not qualitatively match well, and the error between the exact and estimated truncation error decreases at only a second-order rate. Figure 4 compares the maximum truncation error estimate normalized by the maximum exact truncation error for a series of grids. The abscissa plots the grid spacing normalized by the finest grid spacing for 513 nodes. With grid refinement, it is clear that the estimated truncation error for k = 2 and 3 will never accurately represent the exact truncation error since they asymptote to a constant error with mesh refinement. The implications of this observation would mean a minimum polynomial order k is required to accurately estimate truncation error specific to each discretization scheme, and is equal to the highest derivative found in the analytic truncation error.

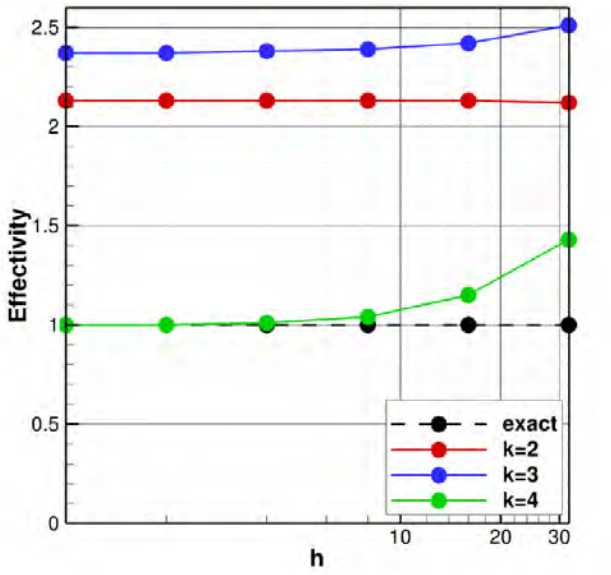

Figure 4. Burgers' equation normalized maximum truncation error estimate vs. grid refinement for Re = 16.

Euler and Navier-Stokes Equations

The same process is applied for the Euler and Navier-Stokes equations as was done for Burgers' equation. The initial goal of this research is to determine the minimum order polynomial reconstruction required to accurately estimate the truncation error for the Euler and Navier-Stokes equations. Solutions and truncation error estimates are computed using three different grid families with the coarsest grid being 17×17 nodes and the finest grid being 257×257 nodes. An example of each is shown in Figure 3. The Cartesian grid is the simplest and is expected to be the easiest to estimate

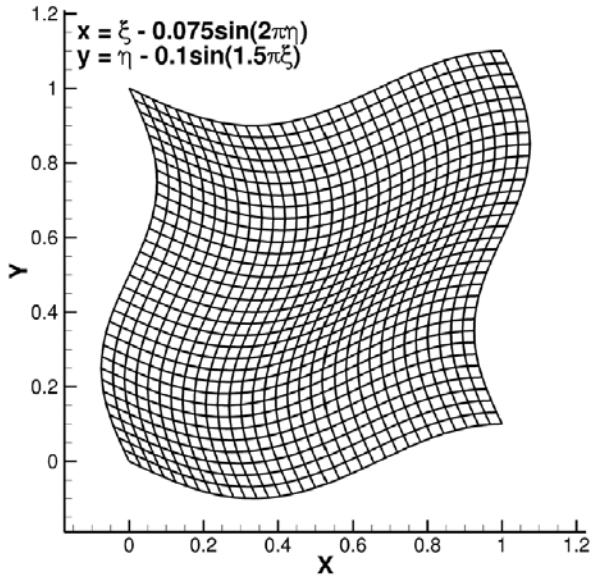

Figure 3. Curvilinear grid, 33×33 grid nodes.

truncation error. The complexity is increased on the skewed grid; however, the linear grid transformation can exactly represent the grid distribution. The final grid is a curvilinear grid with a sinusoidal

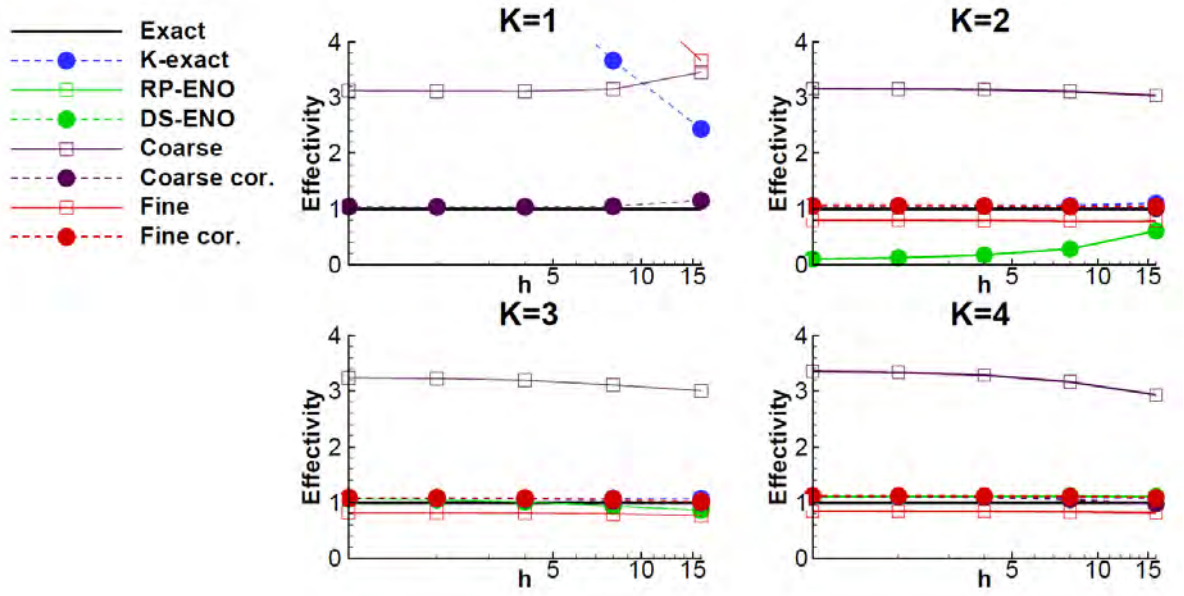

Figure 5. Euler energy truncation error estimation comparisons on the curvilinear mesh for the supersonic solution with a viscosity of μ = 1Pa·s.

distribution which cannot be exactly represented by the linear grid transformation.

Truncation error estimates for Euler and Navier-Stokes solutions are computed using the curvilinear grid. The different methods include k-exact, RP-ENO, DS-ENO, the coarse grid method used by Fulton (2003), with and without the correction term, and the fine grid method used by Venditti and Darmofal (2003), with and without the correction term, for reconstructions with $k = [1,2,3,4]$. The effectivity index (Ainsworth and Oden, 2000) is used to evaluate the truncation error estimates which is the truncation error estimate normalized by the exact truncation error, $\theta_{L2} = \left\|\tau_h(I_h u_h)\right\|_{L2} / \left\|\tau_h(\tilde{u})\right\|_{L2}$. Figure 5 shows the effectivity index for the energy truncation error for the supersonic Euler solution, and Figure 6 shows the effectivity index for the energy truncation error for the subsonic Navier-Stokes solution. The subsonic Euler and Supersonic Navier-Stokes results are very similar to the subsonic Navier-Stokes and supersonic Euler results, respectively. The energy equation was shown because it is the most complex truncation error term; however, the truncation error for the other equations behave in a similar manner.

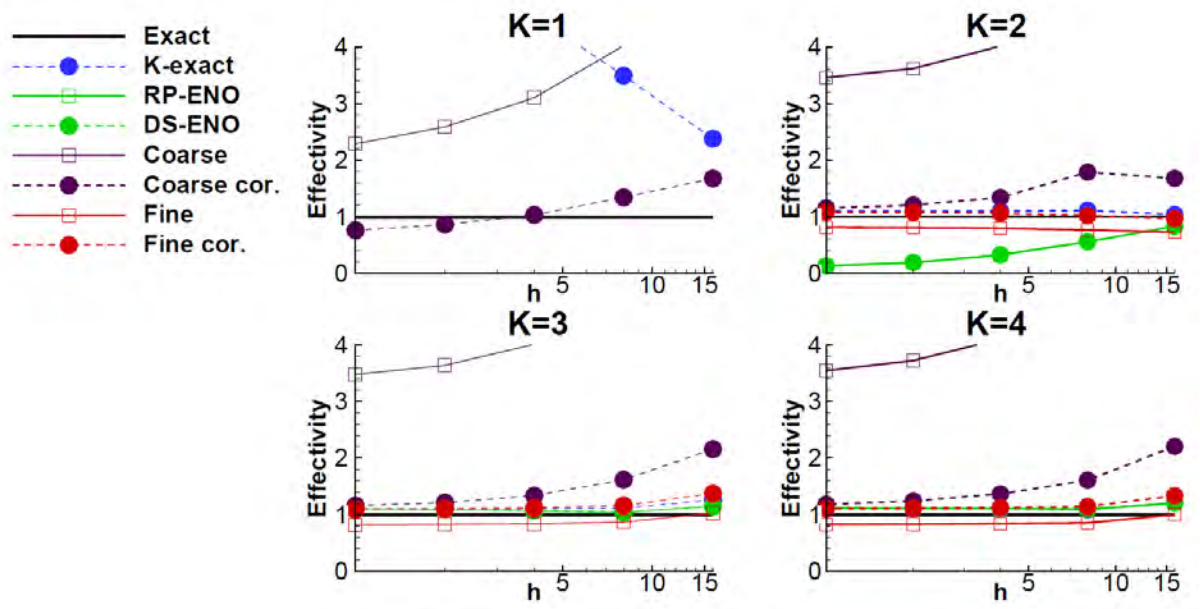

Figure 6. Navier-Stokes energy truncation error estimation comparisons on the curvilinear mesh for the subsonic solution with a viscosity of $\mu = 1$Pa·s.

For both the Euler and Navier-Stokes equations, the k-exact reconstruction method is generally the best performing method. For $k = 1$, the truncation error estimates decrease at a first-order rate where the exact truncation error decreases at a second-order rate. The lower rate results in the estimated truncation error diverging from the exact truncation error with grid refinement. For $k = 2$ and greater, the k-exact truncation error estimates are very accurate and outperform the other methods with only a few exceptions. Based on our previous results with Burgers' equation, it was expected that a higher-order reconstruction would be required for the Navier-Stokes equations; however, all results show that $k = 2$ is sufficient for both the Euler and Navier-Stokes equations. A possible explanation for this result is due to the discretization scheme for the diffusion terms. The derivatives are computed using Green's theorem which reduces to a second-order central difference for one dimensional solutions on an evenly spaced grid. The truncated terms for the second-order central difference is $O(\Delta x^2)$ and $O(\Delta x^4)$. The convective terms have higher order terms which are $O(\Delta x^2)$ and $O(\Delta x^3)$. This would mean that the convective truncation error terms will dominate the error in the truncation error estimate. A higher viscosity Navier-Stokes solution was computed to try to increase the dominance of the diffusive terms. The manufactured solution source terms were compared, and the diffusive terms were on the same order of magnitude as the convective terms. Further evidence that $k = 2$ is sufficient is shown by the divergence of the ENO methods for the supersonic solutions shown in Figure 7 and Figure 8 which are missing derivatives due to the lower dimension reconstruction. If the diffusive terms were insignificant, the ENO methods would be accurate as shown in Figure 7. It might be possible that these terms could dominate for highly diffusive areas of a flow requiring a minimum of $k = 3$; however, there is no evidence to suggest that $k = 2$ is not sufficient.

For the Euler equations and $k = 1$, the ENO truncation error estimation methods decrease at a first-order rate similar to the k-exact method and results in an effectivity index that diverges with grid refinement (not shown in the figure). For $k = 2$, the ENO truncation error estimation methods decrease at a third-order rate resulting in a substantial under prediction of the truncation error. The exact reason for

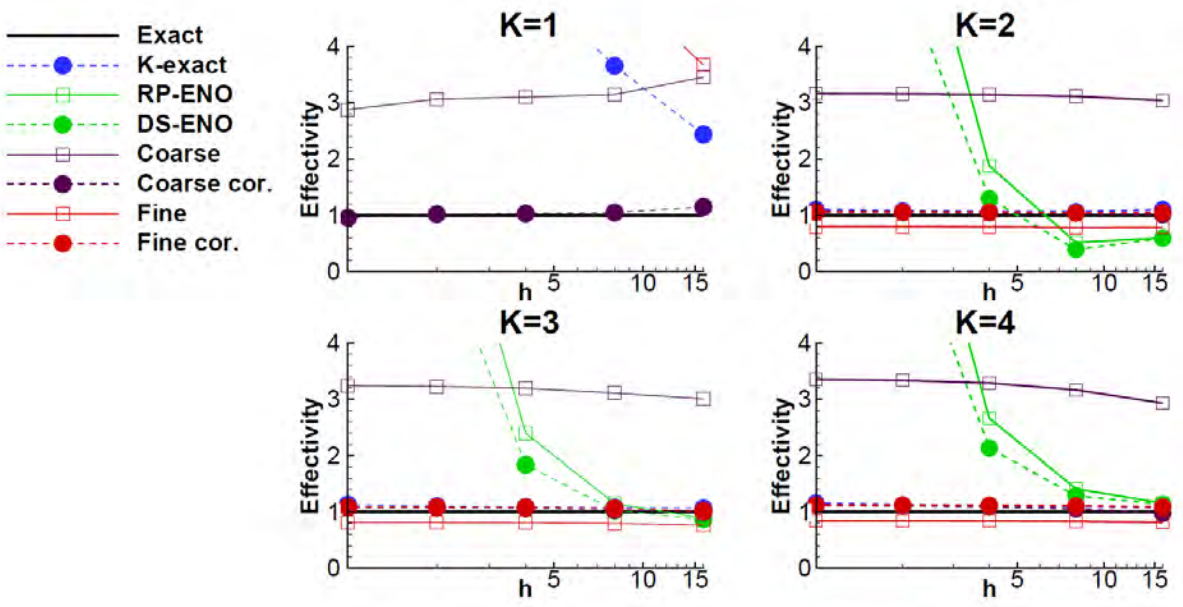

Figure 7. Navier-Stokes energy truncation error estimation comparisons on the curvilinear mesh for the subsonic solution with a viscosity of μ = 1Pa·s.

this behavior is not yet understood; however, the ENO schemes are used for solution reconstruction where $k = 2$ is third order accurate. The truncation error estimate for $k = 2$ could be an estimate of the truncation error not for the current MUSCL extrapolation upwind method but an approximation of the third-order accurate ENO scheme; however, the truncation error estimates for $k = 3$ and $k = 4$ results in accurate truncation error estimates with only slightly higher error than the k-exact method. For the Navier-Stokes equations, the subsonic solution follows a similar trend as the Euler equations; however, for the supersonic solution the ENO methods do not accurately estimate the truncation error. The estimate is zeroth order accurate because the ENO methods cannot represent the cross-derivative terms. The difference between the subsonic and supersonic Navier-Stokes solution (shown in Figure 7) is thought to be due to the relative magnitude of the convective and diffusive terms. The supersonic solution has much larger convective terms due to the larger magnitude velocity and velocity gradient and the zeroth order terms are more apparent. The ENO schemes can be used for truncation error estimation; however, accuracy would suffer in diffusive dominated flow regimes such as boundary layers or shear flows. The effects of a more dominant diffusive term is shown in Figure 8 compared to Figure 7. (Due to stability issues with the higher viscosity, only three grid levels converged iteratively.) The results are similar, except the truncation error estimated from the solution computed with a viscosity of 50Pa·s diverges more quickly than the truncation error estimated from the solution computed with a viscosity of 1Pa·s.

For the coarse grid truncation error estimation methods, solution reconstruction is used to interpolate the coarse grid truncation error estimate back to the computational mesh. The uncorrected coarse grid truncation error estimation method is off by a factor of $1/(r^{p_f} - 1)$; however, the corrected method accurately estimates the truncation error. The most accurate reconstruction scheme for the corrected method uses a k-exact reconstruction method with $k = 1$ for the Euler equations. For the Navier-Stokes

equations, $k = 1$ underestimates the error for the subsonic solution and the more diffusive supersonic solution; therefore, for the Navier-Stokes equations $k = 2$ is recommended.

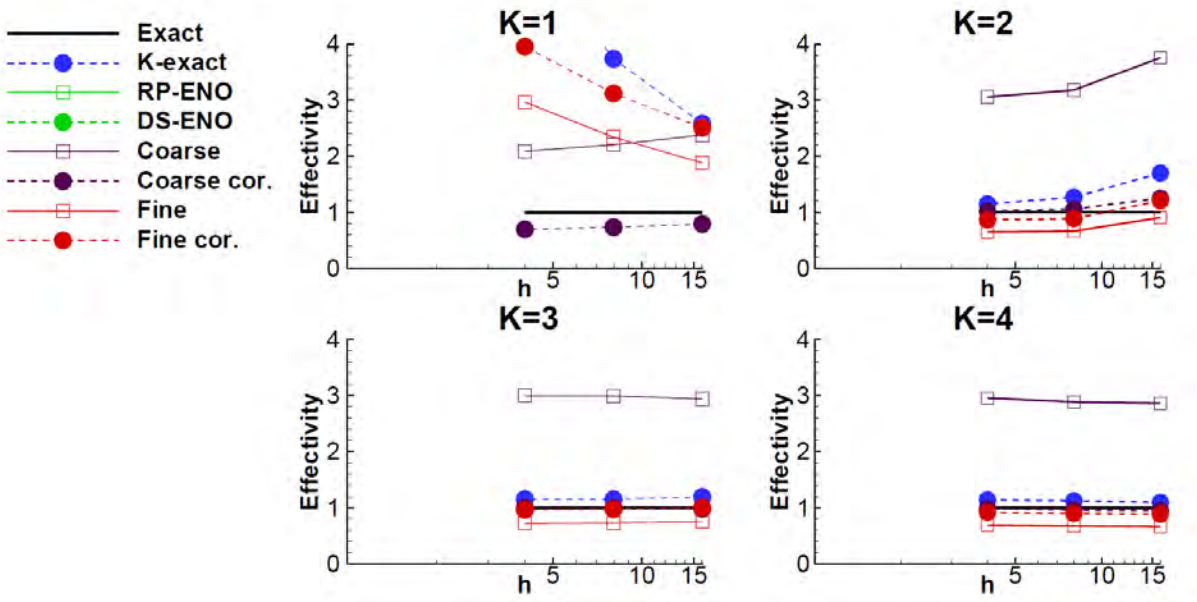

Figure 8. Navier-Stokes energy truncation error estimation comparisons on the curvilinear mesh for the supersonic solution with a viscosity of $\mu = 50$Pa·s.

For the fine grid truncation error estimation methods, solution reconstruction is used to interpolate the computational solution onto a finer mesh that is refined by a factor of two in all coordinate directions. The uncorrected fine grid truncation error estimation method underestimates the truncation error. Corrected by a factor of $r^{p_f}/(r^{p_f}-1)$ results in an accurate truncation error for $k = 2$ or higher for both the Euler equations and the Navier-Stokes equations. The fine grid method with the correction is one of the most accurate truncation error estimators evaluated. The method is more accurate for $k = 2$ than the ENO and coarse grid methods and indistinguishable from the k-exact method for all solutions except the highly diffusive Navier-Stokes solutions in which the k-exact truncation error estimate is more accurate. It is important to note that the test problems are very smooth. The correction term assumes that the truncation error decreases at the formal order of accuracy which may not be the case for highly non-asymptotic solutions, solutions with poor grid quality, or solutions with singularities/discontinuities.

Contour plots of the Navier-Stokes energy truncation error estimates for the supersonic solution on the 33×33 grid are shown in Figure 9. The reconstruction order for each method was chosen from the best results from the previous results shown. All contour plots have the same contour levels. All contour plots compare qualitatively well to the exact truncation error. The k-exact and fine grid method with the correction term compare very well to the exact truncation error. The coarse grid method with the correction factor also compares well but has a few peaks that are not present in the exact truncation error. The ENO methods qualitatively match well, but the truncation error estimates are not as smooth. The truncation error for the ENO methods on the 33×33 grid is the most accurate estimate for the series of grid levels (see Figure 7, $k = 3$). On the 65×65 grid the truncation error estimate begins to diverge.

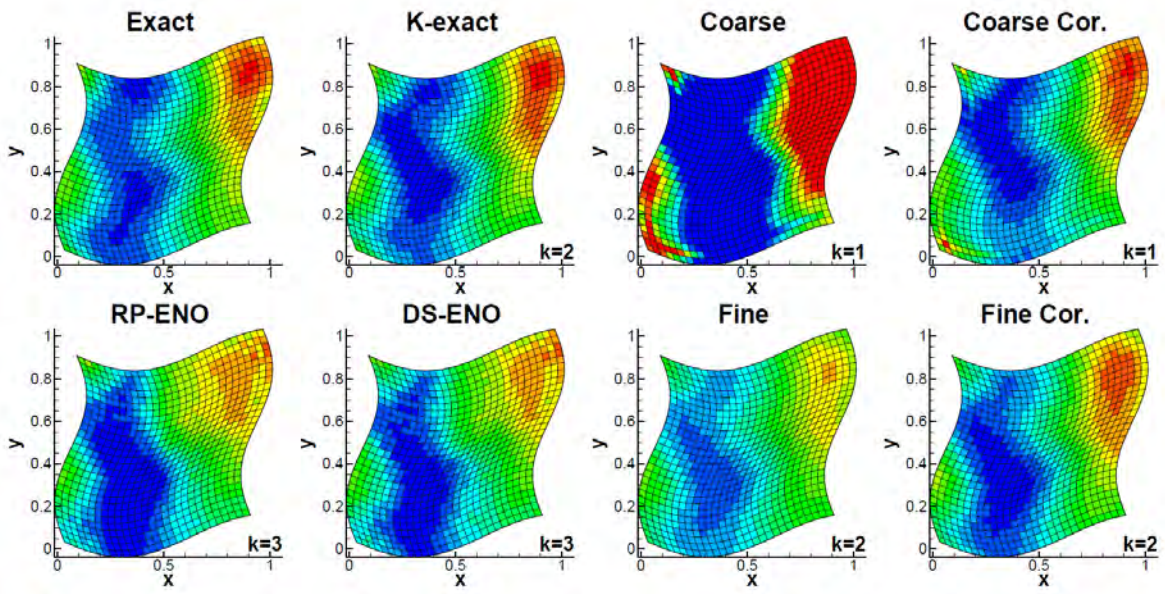

Figure 9. Truncation error estimate contours for Navier-Stokes energy equation on a 33×33 curvilinear grid.

In the presence of shocks, the order of accuracy of the numerical scheme reduces to first-order accurate. The same results were computed for first-order Euler and Navier-Stokes solutions to determine the minimum required reconstruction order for the truncation error estimation methods. The results are shown in Figure 10. The results show that the reconstruction order is one less than what is required for second-order accurate solutions for both the Euler and Navier-Stokes equations. All methods are accurate for $k = 1$ except the ENO schemes which require $k = 2$. The coarse grid correction term reduces to one (i.e., it is not needed) for first-order solutions and the fine grid correction term is two as expected.

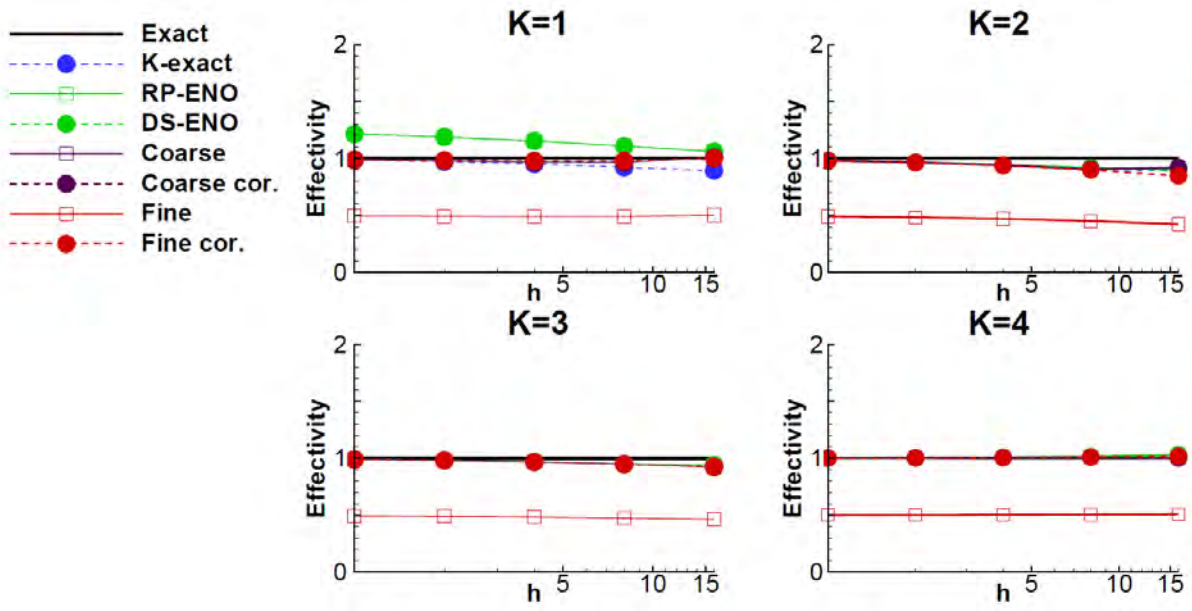

Figure 10. Navier-Stokes energy truncation error estimation comparisons on the curvilinear mesh for the supersonic first-order solution.

The results for all the truncation error estimation methods are summarized as follows. The two best performing methods are the k-exact and the fine grid method with the correction term. The k-exact method does not require the assumption of an order of accuracy which is a significant advantage, especially for more practical applications where the formal order of accuracy may not be achieved. For the first-order accurate methods, the ENO methods minimum required reconstruction order for the Navier-Stokes equations showed $k = 2$ is sufficient. This is because the diffusion terms (evaluated using Green's theorem) are still second-order accurate while the convective terms are first-order accurate. The convective error terms dominate the truncation error and results in truncation error estimates that are nearly identical to the Euler equations. This result suggest that the ENO methods could be used in the vicinity of flow singularities such as shock or contact discontinuities, where the order of accuracy reduces to first order or below (Banks et al., 2008).

There are several uses for truncation error which include discretization error estimation and higher order solution correction. The possible discretization error estimation methods include the error transport equations (Zhang et al., 2002; Qin and Shih, 2002), defect correction (Pereyra, 1965; Stetter, 1978; Skeel, 1986), and adjoint methods (Giles and Pierce, 2000). Defect correction is the least code intrusive to implement as the estimated truncation error is added as a source term, $L_h(\bar{u}) = \tau_h(I_h^k u_h)$. The solution $\bar{u}$ is an estimate of the exact solution, and the discretization error is estimated by $\bar{\varepsilon}_h = u_h - \bar{u}$. An example of defect correction is shown in Figure 11 computed using all truncation error methods for the supersonic Euler solution on the curvilinear grid. A slice is taken through the center of the domain at the $j = 16$ cell index. The k-exact and ENO truncation error estimation methods are the most accurate with the corrected coarse grid method performing well. The uncorrected coarse grid method is not accurate and overestimates the error significantly. The fine grid methods do not capture the shape of the discretization error very well.

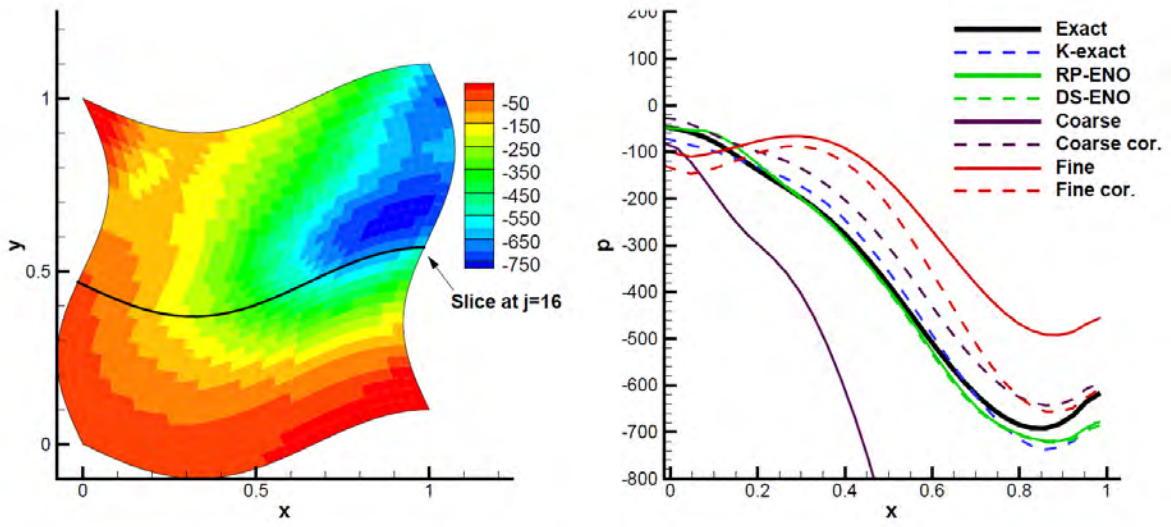

Figure 11. Defect correction example using the supersonic Euler solution on the 33×33 grid.

The second solution $\bar{u}$ is a higher order accurate solution and can be used as a solution instead of estimating the discretization error. Again, for the supersonic Euler equations, the k-exact method is used to compute higher-order solutions shown in Figure 12. The expected order of accuracy is third-order because the k-exact method is estimating the leading truncation error terms which are $O(\Delta x^3)$. The order of accuracy begins very high and appears to be approaching third-order for the finest grid. The higher-order discretization error is not as asymptotic as the second-order solution; however, the discretization error on the finest grid is on the order of 1×10^{-8} % error. The discretization error in the corrected solution is lower for all solution variables except for the pressure which is higher than the second-order solution, but because of the higher order of accuracy quickly decreases. The solver does not have any higher-order capability, the higher-order results come from the truncation error estimate only.

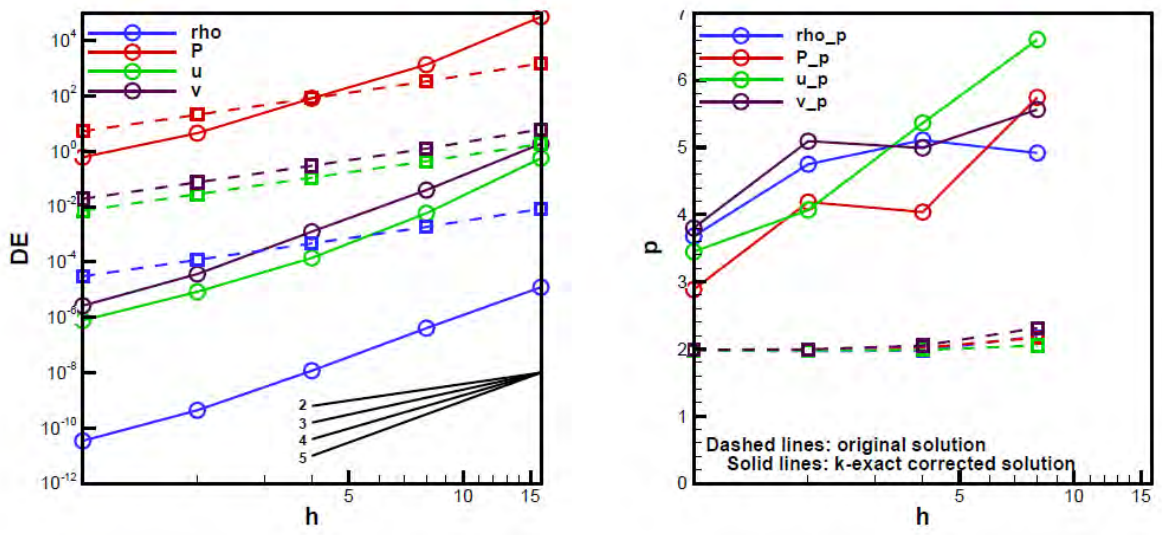

Figure 12. Discretization error in the defect correction solution discretization error (left) and the order of accuracy (right) computed using the k-exact truncation error estimation method for the supersonic Euler solution.

VII. Residual-Based Discretization Error Estimation

In general, the focus of the discretization error estimation is local solution estimation. The local solution variables for the compressible Euler and Navier-Stokes equations are density, pressure, and velocity components. To evaluate the accuracy, contour plots are used; however, for a more quantitative analysis discrete L_1- and L_2-norms are used. The L_1-norm is used when shocks are present in the solution

$$\left\|\varepsilon_h\right\|_{L1} = \frac{1}{N}\sum_{i=1}^{N}\left|\varepsilon_i\right| \tag{37}$$

and the L_2-norm is used otherwise

$$\left\|\varepsilon_h\right\|_{L2} = \sqrt{\frac{1}{N}\sum_{i=1}^{N}\varepsilon_i^2} \tag{38}$$

To compare the estimated errors to the exact errors, the effectivity index is used (Ainsworth and Oden, 2000)

$$\theta_{L2} = \frac{\left\|\bar{\varepsilon}_h\right\|_{L2}}{\left\|\varepsilon_h\right\|_{L2}} \tag{39}$$

where $\bar{\varepsilon}_h$ is an estimated error and ε_h is the exact error. If the estimated error is accurate $\theta_{L2} \approx 1$. For asymptotically accurate error estimates the effectivity index should approach one as the computational grid is refined. The effectivity index is used to evaluate local truncation error and local discretization error estimates for L_1- and L_2-norms where appropriate.

The residual-based discretization error estimation methods that we will investigate include error transport equations, defect correction, and adjoint methods. All three of these methods have both a continuous and a discrete implementation and use discrete or continuous residuals that can be related back

to the truncation error. The error transport equations and defect correction both involve solutions of additional governing equations on the same mesh with residuals/truncation errors acting as local source terms; however, the error transport equations involve an additional linearization step while defect correction relies on the "nearness" of a nearby problem to the original one. Here we reformulate all three residual-based error estimations methods within the new GTEE framework of Equation (10).

Error Transport Equations

Using the new GTEE framework given by Equation (10), the continuous discretization error transport equation can be found as follows. First, insert $I_h u_h$ into the GTEE and subtract the restriction of the PDE ($I^h L(\tilde{u}) = 0$) to give

$$I^h L(I_h u_h) - I^h L(\tilde{u}) = -TE_h(I_h u_h) \tag{40}$$

where we have assumed that $L_h(I^h I_h u_h) = L(u_h) = 0$ (i.e., that the restriction of the prolongation returns the discrete value). Prolonging Equation (40) to a continuous space and making the approximation $I_h I^h L(\tilde{w}) \approx L(\tilde{w})$ (which is not generally true, but may be a reasonable approximation) results in:

$$L(I_h u_h) - L(\tilde{u}) = -I_h TE_h(I_h u_h)\,. \tag{41}$$

If the equations are linear, or if we employ simple linearization, then $L(I_h u_h) - L(\tilde{u}) = L(I_h u_h - \tilde{u}) = L(\varepsilon)$ thus resulting in the continuous discretization error transport equation

$$L(\varepsilon) = -I_h TE_h(I_h u_h) \tag{42}$$

which for our 1D Burgers' equation example becomes:

$$\tilde{u}\frac{d\varepsilon}{dx} - \nu\frac{d^2\varepsilon}{dx^2} = -I_h TE_h(I_h u_h)\,.$$

Here we propose a more advanced linearization by noting that the operators for Burgers' equation in Equation (41) can be written out as

$$L(I_h u_h) - L(\tilde{u}) = I_h u_h \frac{d(I_h u_h)}{dx} - \nu\frac{d^2(I_h u_h)}{dx^2} - \tilde{u}\frac{d\tilde{u}}{dx} - \nu\frac{d^2\tilde{u}}{dx^2}\,. \tag{43}$$

Using the definition of the discretization error from Equation (11) to give $I_h u_h = \tilde{u} + \varepsilon$ and substituting into Equation (43) gives

$$L(I_h u_h) - L(\tilde{u}) = (\tilde{u} + \varepsilon)\frac{d(I_h u_h)}{dx} - \nu\frac{d^2(I_h u_h)}{dx^2} - \tilde{u}\frac{d\tilde{u}}{dx} - \nu\frac{d^2\tilde{u}}{dx^2}$$

or simply

$$L(I_h u_h) - L(\tilde{u}) = \tilde{u}\frac{d\varepsilon}{dx} - \nu\frac{d^2\varepsilon}{dx^2} + \varepsilon\frac{d(I_h u_h)}{dx} = \bar{L}(\varepsilon) + \varepsilon\frac{d(I_h u_h)}{dx}. \tag{44}$$

where the overbar on the PDE operator indicates a linearization. With this advanced linearization, the continuous discretization error transport equation for Burgers' equation becomes

$$\tilde{u}\frac{d\varepsilon}{dx} - \nu\frac{d^2\varepsilon}{dx^2} = -I_h TE_h(I_h u_h) - \varepsilon\frac{d(I_h u_h)}{dx}.$$

It is important to include the additional source term since both the truncation error and the discretization error ε will have the same formal order of accuracy. As will be shown later, omitting this term results in error estimates which are incorrect by a fixed factor (e.g., they are always 30% low regardless of the level of mesh refinement). Shih and Williams (2009) address this linearization issue indirectly by formulating the residual on a finer mesh rather than employing the true truncation error.

A similar discrete discretization error transport equation can be found by inserting $\tilde{u}$ into the GTEE and subtracting the discrete equations ($L_h(u_h) = 0$) to give

$$L_h(u_h) - L_h(I^h\tilde{u}) = -TE_h(\tilde{u}). \tag{45}$$

If the equations are linear, or if we employ a simple linearization, then $L_h(u_h) - L_h(I^h\tilde{u}) = L_h(u_h - I^h\tilde{u}) = L_h(\varepsilon_h)$ thus resulting in the discrete discretization error transport equation

$$L_h(\varepsilon_h) = -TE_h(\tilde{u}) \tag{46}$$

which for the simple 2nd order accurate finite difference discretization of 1D Burgers' equation becomes:

$$u_i\frac{\varepsilon_{i+1} - \varepsilon_{i-1}}{2\Delta x} - \nu\frac{\varepsilon_{i+1} - 2\varepsilon_i + \varepsilon_{i-1}}{\Delta x^2} = -TE_h(\tilde{u}). \tag{47}$$

The more advanced linearization has $L_h(u_h) - L_h(I^h\tilde{u}) = \bar{L}_h(\varepsilon_h) + \varepsilon_i\frac{\tilde{u}_{i+1} - \tilde{u}_{i-1}}{2\Delta x}$ resulting in

$$u_i\frac{\varepsilon_{i+1} - \varepsilon_{i-1}}{2\Delta x} - \nu\frac{\varepsilon_{i+1} - 2\varepsilon_i + \varepsilon_{i-1}}{\Delta x^2} = -TE_h(\tilde{u}) - \varepsilon_i\frac{\tilde{u}_{i+1} - \tilde{u}_{i-1}}{2\Delta x}. \tag{48}$$

Note that the presence of the exact solution to the PDEs in the above error transport equations can always be approximated by the numerical solution and the error estimate: $\tilde{u}_i = I^h\tilde{u} = u_i - \varepsilon_i$.

Since we already have an implicit solution capability in our code, we have found that the following alternative linearization provides an efficient form of the error transport equations. The discrete error transport equations are derived by substituting the exact solution to the continuous governing equation into the GTEE given in (10), subtracting, $L_h(u_h) = 0$, and noting that $L(\tilde{u}) = 0$:

$$L_h(u_h) - L_h(I^h\tilde{u}) = -\tau_h(\tilde{u}) \tag{49}$$

The second term on the left-hand side can be linearized in a Taylor series expanded about the numerical solution u^h:

$$L_h(I^h\tilde{u}) = L_h(u_h) - \bar{\varepsilon}_h \frac{\partial L_h(u_h)}{\partial u} + \frac{\bar{\varepsilon}_h^2}{2}\frac{\partial^2 L_h(u_h)}{\partial u^2} - O(\bar{\varepsilon}_h^3) \tag{50}$$

Inserting this equation into Equation (49), we obtain the final error transport equation result:

$$\frac{\partial L_h(u_h)}{\partial u}\bar{\varepsilon}_h = -\tau_h(I_h u_h) + O(\bar{\varepsilon}_h^2) \tag{51}$$

The derivative is the global Jacobian of the linearized discrete operator which is required to implement an implicit scheme. The Jacobian is commonly available in flow solvers; however, the Jacobian required to solve the error transport equations should be the full higher order (e.g., second-order) left-hand side where only the first-order left-hand side may be required for an implicit solve. The above form of the error transport equation is approximate so the exact discretization error may not result if the exact truncation error is used; however, the error in Equation (51) decreases at a much higher rate and would introduce non-negligible error only in the case of very large discretization errors.

Defect Correction

Defect correction methods were originally developed nearly 50 years ago in order to improve the accuracy of (or estimate the numerical error in) numerical solutions to ordinary differential equations (e.g., Zadunaisky, 1966; Stetter, 1978). More recently, defect correction has been used in CFD to increase the accuracy of 1st order spatial discretization schemes (Layton et al., 2002; Naumovich et al., 2010). We are interested in using defect correction methods to estimate the discretization error in CFD solutions. There are two main types of defect correction (Skeel, 1986): continuous defect correction (also called differential correction) and discrete defect correction (also called difference correction). We will present the main ideas behind our approach to continuous defect correction, then simply explain how discrete defect correction would differ.

Defect correction corrects the original numerical solution by re-solving the original problem with the truncation error estimate added to the right-hand side. Defect correction requires minimal code intrusion. The exact defect correction problem is defined as

$$L_h(I^h\tilde{u}) = \tau_h(\tilde{u}) \tag{52}$$

If the exact truncation error $\tau_h(\tilde{u})$ is added as a source term, the resulting numerical solution is the exact solution to the PDEs or integral equations restricted to the computational grid. Our defect correction implementation takes the form

$$L_h(\bar{u}) = \tau_h(I_h^k u_h) \tag{53}$$

where $\bar{u} \approx \tilde{u}$ and the discretization error estimate is

$$\varepsilon_h \approx \bar{\varepsilon}_h = u_h - \tilde{u}\,. \tag{54}$$

Defect correction requires a second numerical solution on the original computational mesh; however, computational expense is reduced because the original numerical solution to the primal problem is used to initialize the second simulation, thus providing a very good starting solution.

Adjoint Methods

Adjoint methods provide a means by which discretization error estimation and mesh adaptation can be targeted to a solution functional (e.g., lift or drag). We begin our discussion of adjoint methods by reinterpreting adjoint methods in the GTEE framework. Consider a scalar solution functional $J(\tilde{u})$ and its discrete counterpart $J_h(u_h)$. We may be interested in estimating the discretization error in this functional

$$\varepsilon_h = J_h(u_h) - J(\tilde{u}), \tag{55}$$

assessing the sensitivity of this functional to local values of the truncation error, or both. For the continuous adjoint, we first form the Lagrangian using the inner product (e.g., $\langle f, g \rangle = \int_a^b f(x)g(x)dx$)

$$\ell(\tilde{u}, \Psi) = J(\tilde{u}) - \langle \Psi, L(\tilde{u}) \rangle \tag{56}$$

Next, linearize both *J* and *L* about the general function *u*:

$$J(\tilde{u}) = J(u) + \left.\frac{\partial J}{\partial u}\right|_u (\tilde{u} - u) + HOT \qquad \text{and} \qquad L(\tilde{u}) = L(u) + \left.\frac{\partial L}{\partial u}\right|_u (\tilde{u} - u) + HOT \ .$$

Inserting these linearizations into the right-hand side of Equation (56) and neglecting the higher-order terms gives

$$\ell(\tilde{u}, \Psi) = J(u) - \langle \Psi, L(u) \rangle + \left[\left.\frac{\partial J}{\partial u}\right|_u - \left\langle \Psi, \left.\frac{\partial L}{\partial u}\right|_u \right\rangle \right] (\tilde{u} - u) \ . \tag{57}$$

Replacing the general function *u* in Equation (57) with the prolongation of a numerical solution, i.e., $u = I_h u_h$, we have

$$\ell(\tilde{u}, \Psi) = J(I_h u_h) - \langle \Psi, L(I_h u_h) \rangle + \left[\left.\frac{\partial J}{\partial u}\right|_{I_h u_h} - \left\langle \Psi, \left.\frac{\partial L}{\partial u}\right|_{I_h u_h} \right\rangle \right] (\tilde{u} - I_h u_h) \tag{58}$$

where the adjoint (dual) problem is defined as

$$\left.\frac{\partial J}{\partial u}\right|_{I_h u_h} = \left\langle \Psi, \left.\frac{\partial L}{\partial u}\right|_{I_h u_h} \right\rangle . \tag{59}$$

Once the adjoint problem is solved for Ψ, the term in brackets in Equation (58) will be equal to zero. By noting that the PDE is equal to zero over the entire domain (i.e., $L(\tilde{u}) = 0$), we can use Equation (56) to replace the Lagrangian with $\ell(\tilde{u}, \Psi) = J(\tilde{u})$ in Equation (58) to give

$$J(I_h u_h) - J(\tilde{u}) = \left\langle \Psi, L(I_h u_h) \right\rangle \tag{60}$$

where $L(I_h u_h)$ is simply the continuous residual (an estimate of the truncation error). If the functional J involves an integral, then the numerical integration errors can be estimated as

$$\varepsilon_{integ} = J_h(u_h) - J(I_h u_h) . \tag{61}$$

Combining Equations (60) and (61) with the definition of the discretization error in the functional given by Equation (55), we have

$$\varepsilon_h = J_h(u_h) - J(\tilde{u}) = J_h(u_h) - J(I_h u_h) + J(I_h u_h) - J(\tilde{u}) = \varepsilon_{integ} + \left\langle \Psi, L(I_h u_h) \right\rangle$$

or simply

$$\varepsilon_h = J_h(u_h) - J(\tilde{u}) = \varepsilon_{integ} + \left\langle \Psi,\ L(I_h u_h) \right\rangle . \tag{62}$$

The discretization error in the solution functional is thus due to 1) the integration error (which can be reduced simply by improving the numerical quadrature used in evaluating the integral) and 2) the local truncation error (or residual) weighted by the adjoint sensitivities Ψ. The solution to the adjoint problem thus provides the sensitivity of the solution functional to local truncation error sources. A discrete adjoint could be derived similarly which uses the discrete residual:

$$\varepsilon_h = J_h(u_h) - J(\tilde{u}) = \varepsilon_{integ} - \Psi^T L_h(I^h \tilde{u}) \tag{63}$$

where Ψ^T is a row vector containing the adjoint sensitivities and $L_h(I^h \tilde{u})$ is a column vector containing the local discrete residual (i.e., the truncation error) for each cell in the mesh. Both the continuous and discrete forms of the adjoint method will be investigated within the GTEE framework. Methods for formulating the sensitivities needed for the adjoint methods will be examined including analytical derivative evaluation, numerical derivative evaluation, and complex numbers (Squire and Trapp, 1998).

VIII. Local Error Estimation Results

Local Error Estimates: NACA 0012 Airfoil

For the local error estimates, the truncation error is estimated using the k-exact, least squares (LSQ), DSENO single grid methods as well as the coarse grid method (with and without the correction term) and the fine grid method (with and without the correction term). Defect correction and ETEs are solved with each of the truncation error estimates.

The truncation error estimates for the subsonic airfoil at zero degrees angle of attack are shown in Figure 14. The k-exact and fine grid method with the correction term capture the truncation error around the leading edge of the airfoil. The least squares method compares well also with the exception of a large truncation error estimate at the leading edge. The DS-ENO method results in a very noisy truncation error estimate. The discretization error in pressure is shown in Figure 13. The accuracy of the truncation error estimates directly correspond to the accuracy of the discretization error estimate. The k-exact estimate compares well to the exact discretization error and the DS-ENO method is relatively noisy.

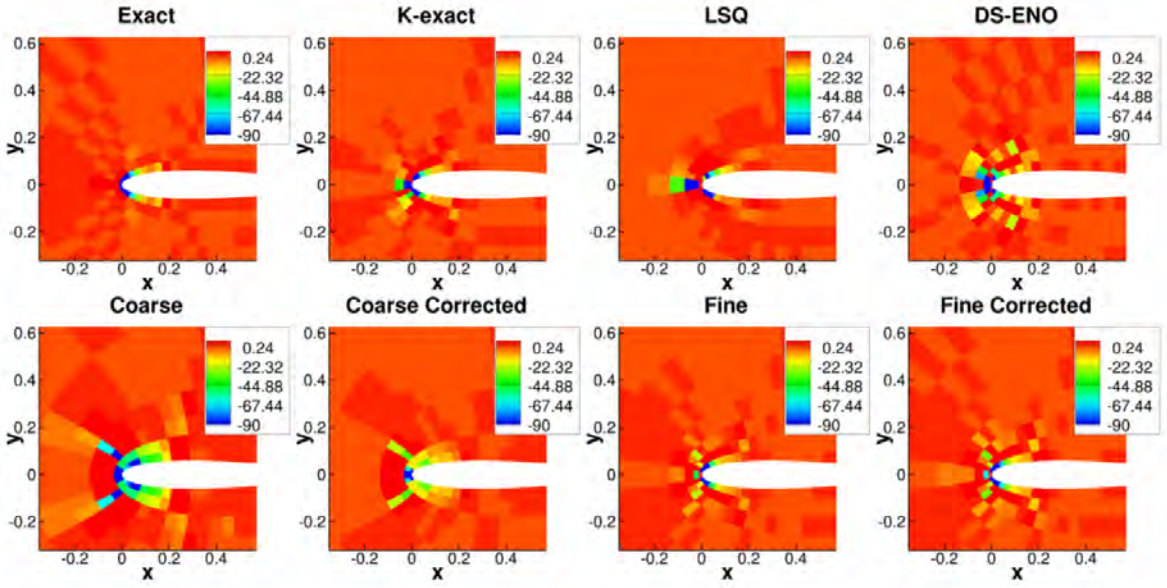

Figure 14. Estimated truncation error for the mass eqn. for the NACA 0012 airfoil at M=0.5 and α=0.

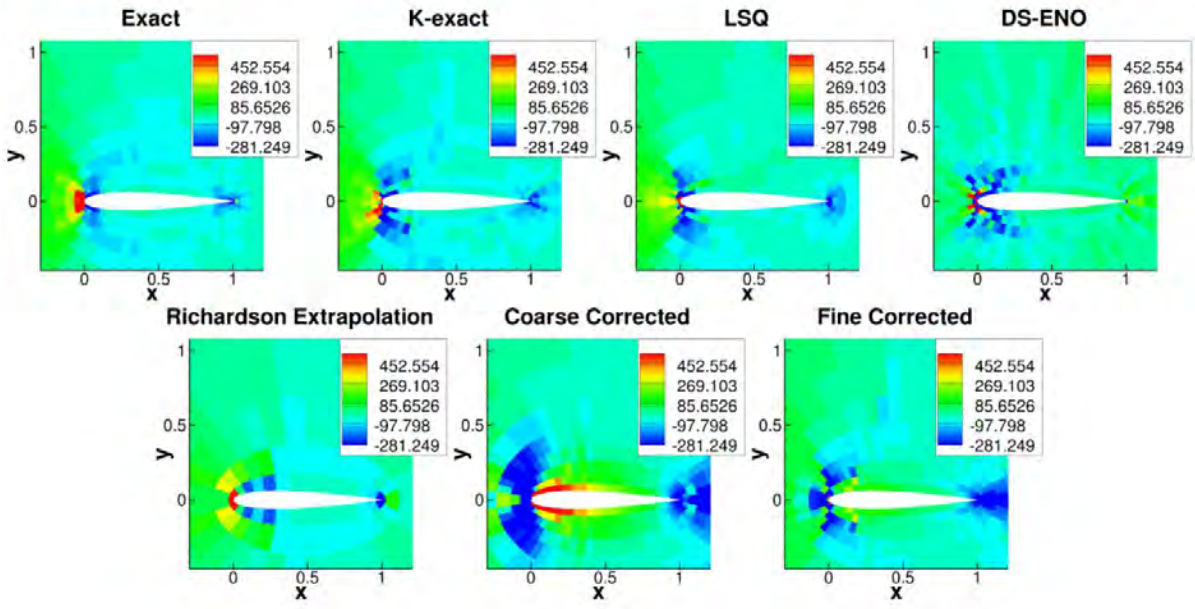

Figure 13. Estimated defect correction discretization error estimates for pressure for the NACA 0012 airfoil at M=0.5 and α=0.

To compare the difference between defect correction and the ETEs, the exact, defect correction estimate, and two ETE estimates are shown in Figure 15. One ETE estimate is computed using a Jacobian computed for first-order discrete equations and the other is computed using a Jacobian computed for the second order discrete equations. The results are very nearly identical and only differ by fractions of a percent. The pressure on the upper wall is also compared in Figure 16. The results are nearly identical for the ETE estimates. The result is fortuitous because a first order Jacobian is often readily available when using an implicit solver. The solution time for the ETEs using the first order Jacobian is negligible compared to the expense of the defect correction estimate. For comparison, the primal solution took 24 minutes while using the k-exact truncation error estimation method, the defect correction error estimate requires about nine minutes to solve while the first-order ETE took less than a second to compute with three iterations. The second-order ETE cost about five seconds to compute with seven iterations. The first-order ETE is so inexpensive because the equations are linear. The difference between the first- and second-order ETE is negligible for all applications so only the first-order ETE results are shown. The ETE estimates slightly underestimate the discretization error at the leading edge compared to defect correction. Both residual-based methods accurately estimate the discretization error while Richardson extrapolation misses the sign and magnitude near the leading edge significantly.

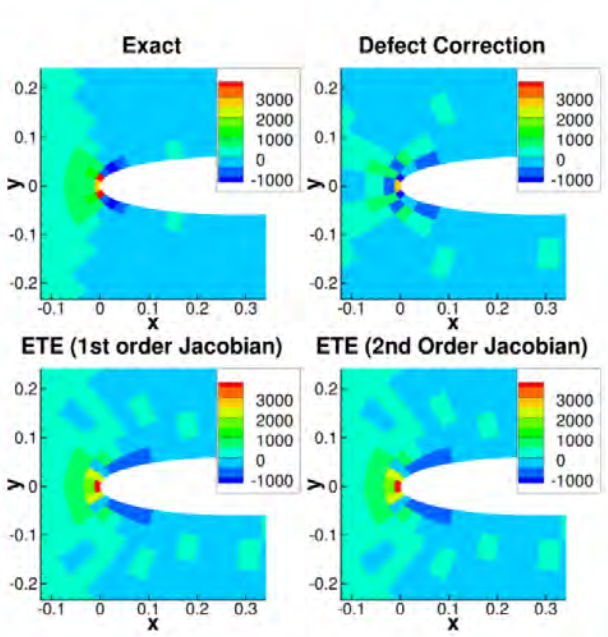

Figure 15. Estimated defect correction and ETE discretization error estimates for pressure for the NACA 0012 airfoil at M=0.5 and α=0 using the k-exact reconstruction method (solid is the benchmark solution).

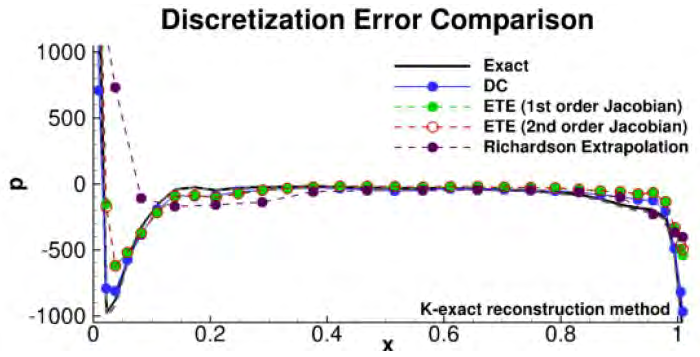

Figure 16. Estimated defect correction and ETE discretization error estimates for pressure along the upper side of the the NACA 0012 airfoil at M=0.5 and α=0 using the k-exact reconstruction method (solid is the benchmark solution).

Figure 17 and Figure 18 compare the pressure on the wall for defect correction and ETE discretization error estimates compared to the exact discretization error. For all cases, the ETE estimate compares well to the defect correction estimate. There are slight differences near discretization error peaks, and overall, the defect correction estimate is more accurate because the estimate results from nonlinear equations compared to the linearized ETEs. In terms of truncation error estimation, the k-exact method is the most accurate with only a minor difference in peak error near the leading edge. The LSQ, DS-ENO, and fine grid method with the correction factor compare well for the entire airfoil with larger differences near the leading edge of the airfoil. All methods compare better than Richardson extrapolation except for the coarse grid methods which are inaccurate over the entire airfoil.

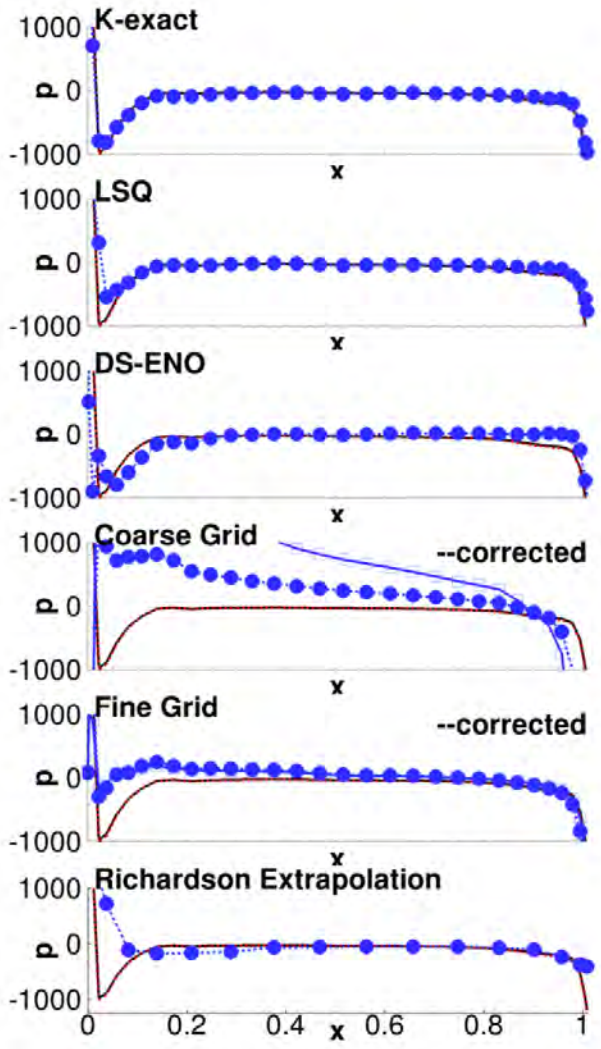

Figure 17. Estimated defect correction discretization error estimates for pressure along the upper side of the NACA 0012 airfoil at M=0.5 and α=0 (solid is the benchmark solution).

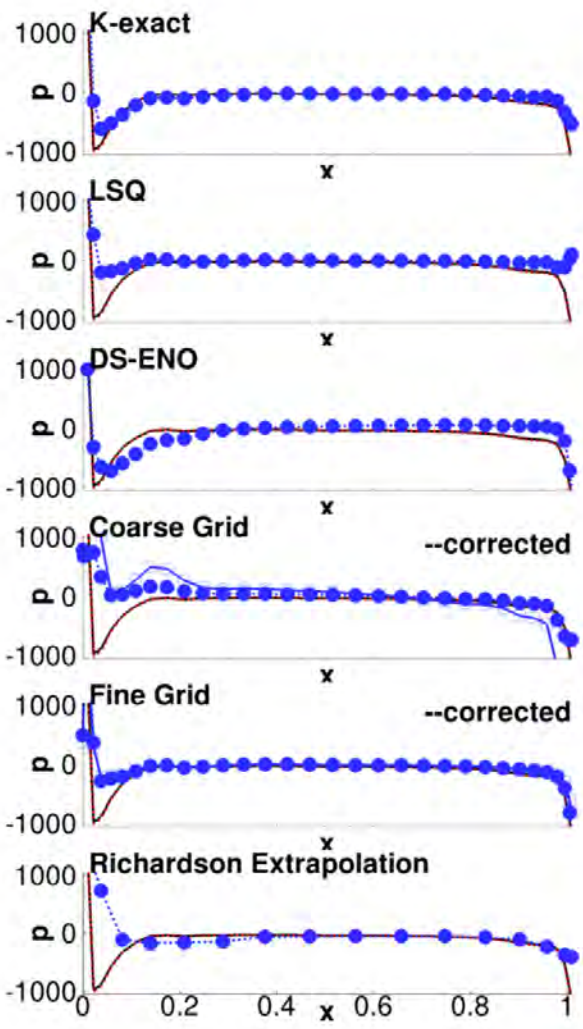

Figure 18. Estimated ETE discretization error estimates for pressure along the upper side of the NACA 0012 airfoil at M=0.5 and α=0 (solid is the benchmark solution).

IX. Functional Error Estimation Results

As alternatives to the adjoint method, which can only provide a DE for a single functional output per dual solve, both defect correction methods (DC) (Pereyra, 1965, 1967, 1968) and the error transport equations (ETEs) (Phillips and Roy, 2011) provide local DE estimates driven by TE estimates and can be used to estimate error in any functional of interest for a single solve. DC methods treat the TE estimate as a source term to drive the primal solver towards a higher order solution. This TE source term can be thought of in a similar manner to the source term utilized by the method of manufactured solutions (MMS) (Roache, 2009; Oberkampf and Roy, 2010) to drive the discrete governing equations towards a preselected solution. If the exact TE is known, then the discrete governing equations can be driven towards computing the exact solution of the continuous governing equations. In practice, the TE is approximated and the computed solution should converge towards the continuous solution at a higher

order rate. DC methods are extremely simple to implement as they only require the formulation of the TE estimate and the ability to include a source term in the discrete solver. In addition, DC methods are generally much less costly to solve than the original discrete system as they can be initialized using the already available discrete solution.

For the results given below, the quasi-1D Euler equations are solved using a MUSCL scheme (van Leer, 1979) with $\kappa = 1/3$ (corresponding to parabolic reconstructions on a Cartesian mesh), the van Albada flux limiter (van Albada et al., 1982), and Roe's approximate Riemann solver flux scheme (Roe, 1981). The Mach number distributions and nozzle geometry are shown in Figure 19 for inflow stagnation conditions of $p_o = 300$ kPa and $T_o = 600$ K. The nozzle is described by a Gaussian bump that avoids curvature discontinuities that can cause TE spikes:

$$A(x) = 1.0 - 0.8\exp\left[-\left(\frac{5^2 x^2}{2}\right)\right], \qquad -1 \le x \le 1.. \tag{64}$$

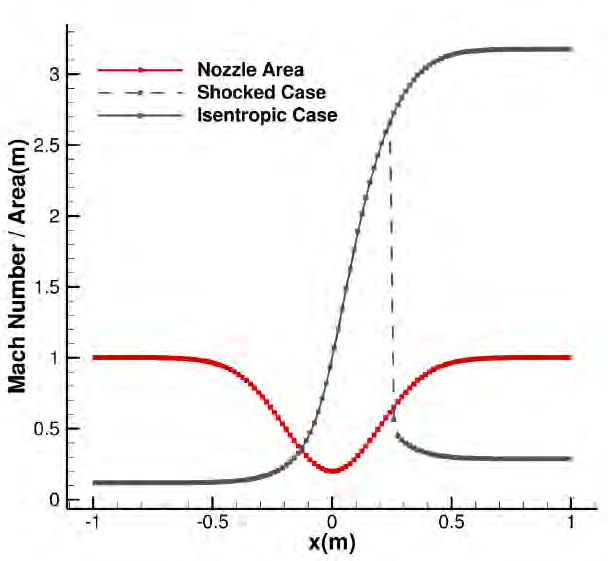

Figure 19. Quasi-1D nozzle area and Mach number distributions.

The functional of interest for the adjoint error estimation is the integral of pressure along the nozzle normalized by the inflow stagnation pressure as given by:

$$\int_{-1}^{1}\left(p/p_o\right)dx\,. \tag{65}$$

and has a value of 1.0187219 for the isentropic case and 1.2972908 for the shocked case as calculated using a seven point Gauss quadrature of the analytic solution on a grid with approximately 1 million cells. For the discrete value of the integral, the trapezoidal rule is applied to the reconstructed solution.

Figure 20a shows the behavior of the base solution error and remaining error after adjoint correction for the functional using the exact TE, the weak estimate of the TE, the embedded grid approach, and the corrected embedded grid approach on a series of Cartesian meshes. As expected, the base error converges at a second order rate. The standard embedded grid approach only demonstrates a half order of magnitude

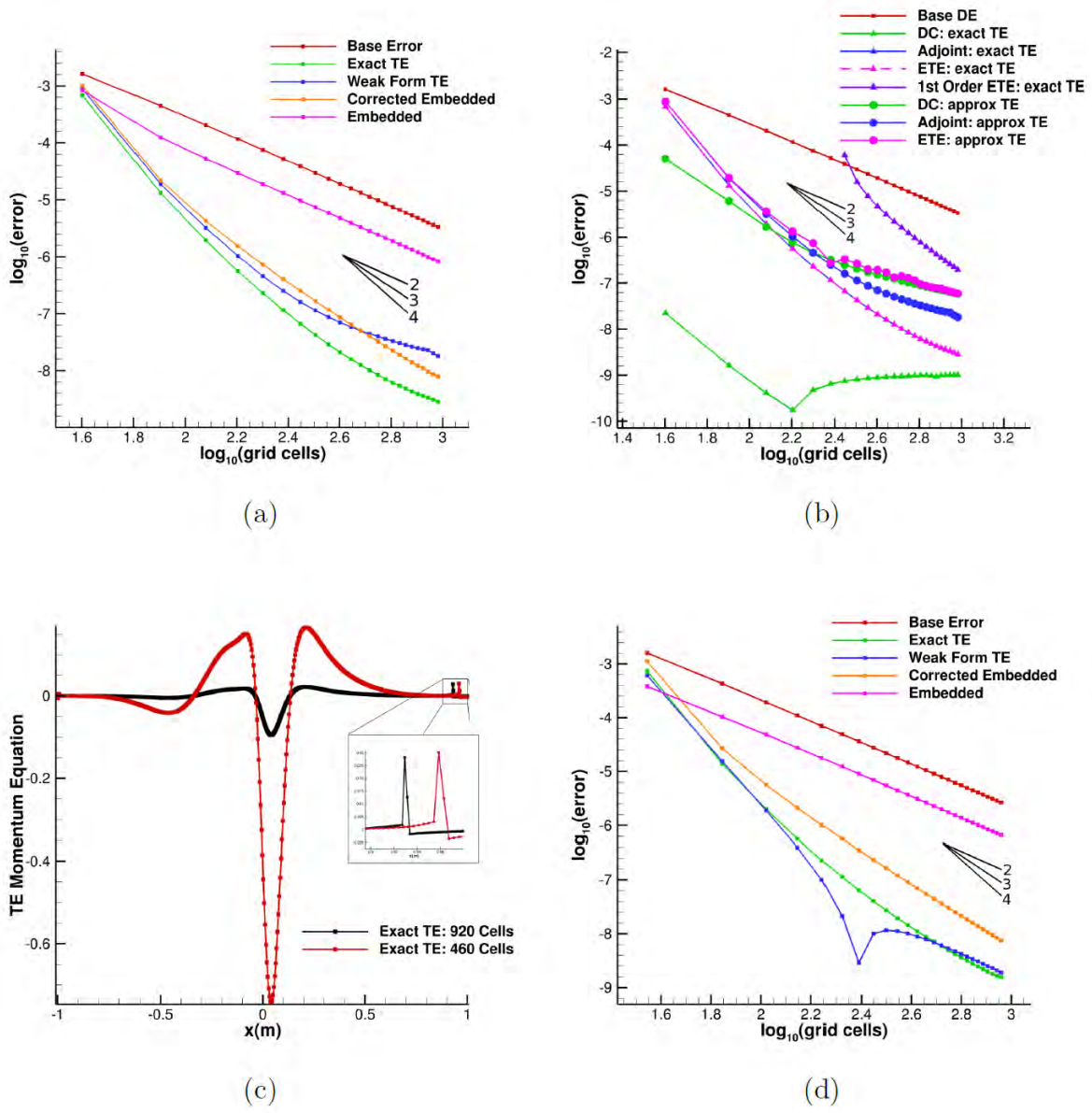

Figure 20. Functional base error and remaining error for isentropic expansion for the adjoint method with various TE estimation techniques (a) and for the adjoint, DC, and ETEs in (b). Note the difference in scales. Demonstration of sign change in TE causing TE spike (c) and functional base error and remaining error for cropped domain which removes the TE spike (d).

reduction in the remaining error with a second order convergence rate, a result seen elsewhere in literature (Nemec and Aftosmis, 2007). For the exact TE and weak form estimate, the remaining error converges at an approximately third to fourth order rate, before beginning to level off towards a first to second order

rate at finer grid levels. The corrected embedded grid method shows a third order convergence rate and surpasses the weak form TE estimate in a region where the weak form begins to demonstrate first order convergence. This lower order convergence is due to a sign change in the TE which creates a zeroth order spike in the TE, as shown in Figure 20c near x = 0.95m. The discrete residual includes a limiter function which smooths out this oscillation in the embedded grid TE estimate and prevents it from dominating the error estimate. If the domain is shortened to remove the region which contains the TE spike, then the performance of the weak form based adjoint error estimate is improved, as shown in Figure 20d, but it now demonstrates a scalloped region due to a change in the sign of the predicted remaining error. It should be noted that the results of Figure 20d are obtained through new solutions of the primal and dual problems on the shortened domain instead of simply removing the contributions of the adjoint weighted TE from the cropped region of the domain.

Comparisons between the ETEs, DC, and the adjoint method are made in Figure 20b. Most notably, when the exact TE is used, the DC essentially returns the exact functional value, and the ETEs and adjoint method converge exactly the same. The better performance of the DC method can be attributed to the fact that it is solving the nonlinear governing equations, while both the adjoint and ETEs are solving linearized problems. A lower order approximation for the ETEs is included where the linearized equations only consists of first order Jacobians. On coarser meshes, the low order formulation of the ETEs will not converge and perform about two orders of magnitude worse than the fully linearized ETEs on the finest mesh. When an approximate TE estimate is used, in this case it is the weak formulation discussed above, the ETEs, DC, and the adjoint method all perform similarly well, but the DC does outperform the others on the coarser mesh levels. Given the similarity in performance, it appears that either the DC method or ETEs could be used in place of an adjoint method in order to provide functional error estimates. Results for the first order ETEs are not included for the approximate TE method as the DE estimates were much worse than the rest.

X. Mesh Adaptation

Introduction

Performing mesh adaptation involves two distinct aspects: choosing a method for driving the adaptation and choosing a mechanism to actually perform the adaptation. While this report is clearly focused on the former, here we briefly mention the mechanism for performing the adaptation that was used. As discussed before, we limited the scope of this effort by demonstrating our error control techniques on structured meshes. Since h-adaptation is not possible on structured meshes, r-adaptation (i.e., mesh movement) was used. Simple spring analogy and elliptical adaptation methods (Baker, 1997) can be used when only a single adaptation driver function is available (e.g., the total truncation error). When more detailed information is available regarding mesh quality contributions, then the spring analogy approach can be supplemented with torsional springs to mitigate skewness effects (e.g., Nakahashi and Deiwert, 1986). Furthermore, variational methods allow for mesh adaptation with the addition of mesh quality constraints (e.g., Lapenta, 2003).

Our approach for driving the mesh adaptation is focused on the residual/truncation error, including adjoint weighting when specific solution functionals are of interest. We maintain that the residual/truncation error is the only theoretically sound approach to driving mesh adaptation. Adaptation based on solution features has been shown to fail (Dwight, 2008), sometimes “disastrously” (Ainsworth

and Oden, 2000). Adaptation based on the discretization error neglects the effects of error transport from other regions of the domain (e.g., through convection and diffusion) and has also been shown to be a poor driver for mesh adaptation (e.g., Gu and Shih, 2001). Adaptation based on recovery-based error estimates (e.g., Zienkiewicz and Zhu, 1992) has seen some success for linear elliptic problems in finite elements, but this success is not expected to carry over to hyperbolic problems using finite difference or finite volume methods.

When the truncation error is available (e.g., from a continuous or discrete residual), then it can be used directly to drive the adaptation process. We explored different methods for assembling the truncation error for each conservation equation (mass, momentum, and energy) into a single weighting function to drive adaptation. Since each conservation equation has different magnitudes (e.g., mass equation versus total energy equation), we investigated methods for scaling the truncation error based on appropriate reference truncation error values from a baseline (i.e., unadapted) mesh. Once this weight function is assembled, appropriate smoothing or filtering methods are used to provide for smooth adaptation. Limiting of the weighting function is also needed to prevent small values (which can occur when the truncation error goes from positive to negative) from affecting the adaptation process. For example, spring-based adaptation when two nodes are connected with a spring with near zero spring constant can result in large local mesh deformations and result in mesh crossover. When one is instead interested in targeted mesh adaptation (i.e., mesh adaptation to reduce the error in a chosen solution functional), then the adjoint solution provides the appropriate weighting for how the local cell's residual/truncation error will affect the functional. For example, instead of adapting the mesh purely on the magnitude of the truncation error, one might instead adapt the mesh based on the truncation error weighted by the adjoint solution.

When conducting adaptation, it is important to monitor the convergence of the adaptation scheme to know when to stop adaptation. However, an appropriate adaptation monitor must be selected that is consistent with the adaptation schemes being used in order to do this. For this investigation, two adaptation monitors are selected based upon the concept of equidistribution. The first adaptation monitor is a truncation error metric given by Equation (66) which compares the L_2 norm of truncation error on the adapted grid to the L_2 norm of truncation error on the initial grid. The L_2 norm of truncation error in 2D is given by Equation (67) where p is equal to 2, $\phi_{i,j}$ represents the truncation error in a given cell, $A_{i,j}$ is the area of a given cell, and A is the total area of the domain.

$$\frac{\left\| TE_{i,j}^{k} \right\|_{2,adapted}}{\left\| TE_{i,j}^{k} \right\|_{2,initial}} \tag{66}$$

$$L_p = \left[\frac{1}{A} \sum_{i=1}^{imax} \sum_{j=1}^{jmax} A_{i,j} \left| \phi_{i,j} \right|^p \right]^{1/p} . \tag{67}$$

The second adaptation monitor is the weight function equidistribution error given by Equation (68) and is taken from previous work by Choudhary (2014):

$$WEE_{i,j} = \left| \frac{\sigma - \left| W_{i,j} \right| A_{i,j}}{\sigma} \right| . \tag{68}$$

where σ is the equidistributed value of the quantity weight function times cell area across the entire computational domain. For all test cases in this study, the convergence tolerance for these adaptation monitors was set to 0.1. Beyond the tolerance of 0.1, mesh movement is minimal and the benefit of further adaptation does not outweigh the added computational cost.

Since truncation error is used as the driver for adaptation, it is necessary to formulate a weight function in terms of truncation error. To holistically adapt the mesh for the entire system, the truncation error from each governing equation must be combined in a consistent manner. This is accomplished by defining the local weight function as the average of the absolute value of each equation's truncation error normalized by its maximum absolute value on the initial or uniform grid. This is given by Equation (69) where *neq* is the number of governing equations in the system:

$$W_{i,j} = \frac{1}{neq} \sum_{k=1}^{neq} \frac{\left| TE_{i,j}^{k} \right|}{\max \left| TE^{k} \right|_{initial}} . \tag{69}$$

When constructing the weight function in this fashion, often there is some amount of high frequency noise present. To prevent the adaptation schemes from diverging or causing mesh crossover, it is necessary to apply a smoothing algorithm to the weight function prior to its application. Weight function smoothing is accomplished by applying the elliptic smoother given in Equation (70):

$$W_{i,j}^{smooth} = \frac{W_{i-1,j} + W_{i+1,j} + W_{i,j-1} + W_{i,j+1} + 8W_{i,j}}{12} . \tag{70}$$

Although some weight function smoothing is required, it is also important that the weight function is not oversmoothed. If the weight function is over-smoothed, information about the problem is lost, and the amount of discretization error improvement will likely be diminished.

Adaptation Results

This report examines the effectiveness of several 2-D r-adaptation schemes in reducing discretization error in numerical solutions. The adaptation schemes used include an adaptive Poisson grid generator (Anderson, 1990), a variational grid generator (Brackbill and Saltzman, 1982), a center of mass based scheme (Laflin, 1997), and a scheme based on deforming maps (Liao and Anderson, 1992). These schemes are applied to Mach 1.2 flow around a 12 deg. downward turn. Discretization error is computed using the known exact solution. Discretization error reductions of up to thirteen times are achieved on adapted grids relative to the discretization error present on a uniform grid of the same size. This error reduction results in a high degree of efficiency since the primal problem converges at a sublinear rate (i.e., less than first order) as expected (Banks et al., 2008).

The test problem is a 2D supersonic expansion fan generated by a Mach 1.2 flow around a 12° downward turn. Three instances of this problem are examined and will be denoted as the "edge case," the "corner case," and the "shifted case." The computational domain for these cases can be found in Figure 21. The grid for each case setup is a 65×65 node grid extending from 0 m to 1 m in both the *x* and *y* directions. The inflow conditions for all cases are static pressure and temperature of 100 kPa and 273 K, respectively.

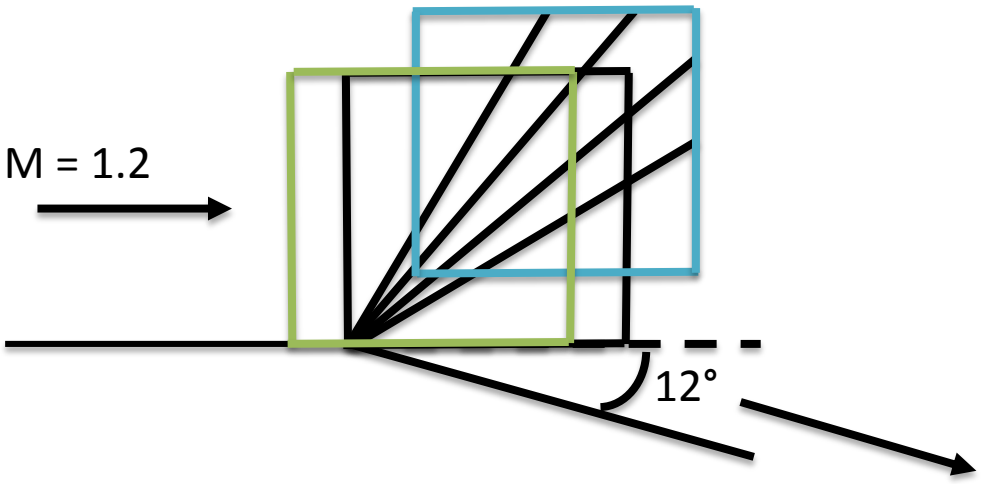

Figure 21. Supersonic expansion fan domains: black square denotes the corner case, blue square denotes the edge case, and the green square denotes the shifted case.

Edge Case

Truncation error and discretization error improvements for the edge case of the supersonic expansion fan achieved by each adaptation scheme may be found in Tyson et al. (2015). In the best case, truncation error is decreased by a factor of ten when using the center of mass approach (Laflin, 1997). For the same adaptation scheme, discretization error is reduced by a factor of six. Anderson's adaptation scheme (Anderson, 1990) also performs well by achieving a six time improvement in discretization error. The Brackbill and Saltzman (1982) and Deformation (Liao and Anderson, 1992) adaptation schemes still achieve some amount of discretization error reduction, but at best it is half the reduction seen with the other two methods.

Qualitative results of truncation error and discretization error reductions for the edge case of the supersonic expansion fan are presented in Figure 22 and Figure 23, respectively. Truncation error results are only presented for the x-momentum equation while discretization error results are only presented for pressure. For this case, the majority of truncation error is located at the beginning and end of the expansion fan, as seen in Figure 22e. Since truncation error is high in these regions of the domain, the adaptation schemes pull nodes to the beginning and end of the expansion fan as illustrated by the adapted grids in Figure 22a - Figure 22d.

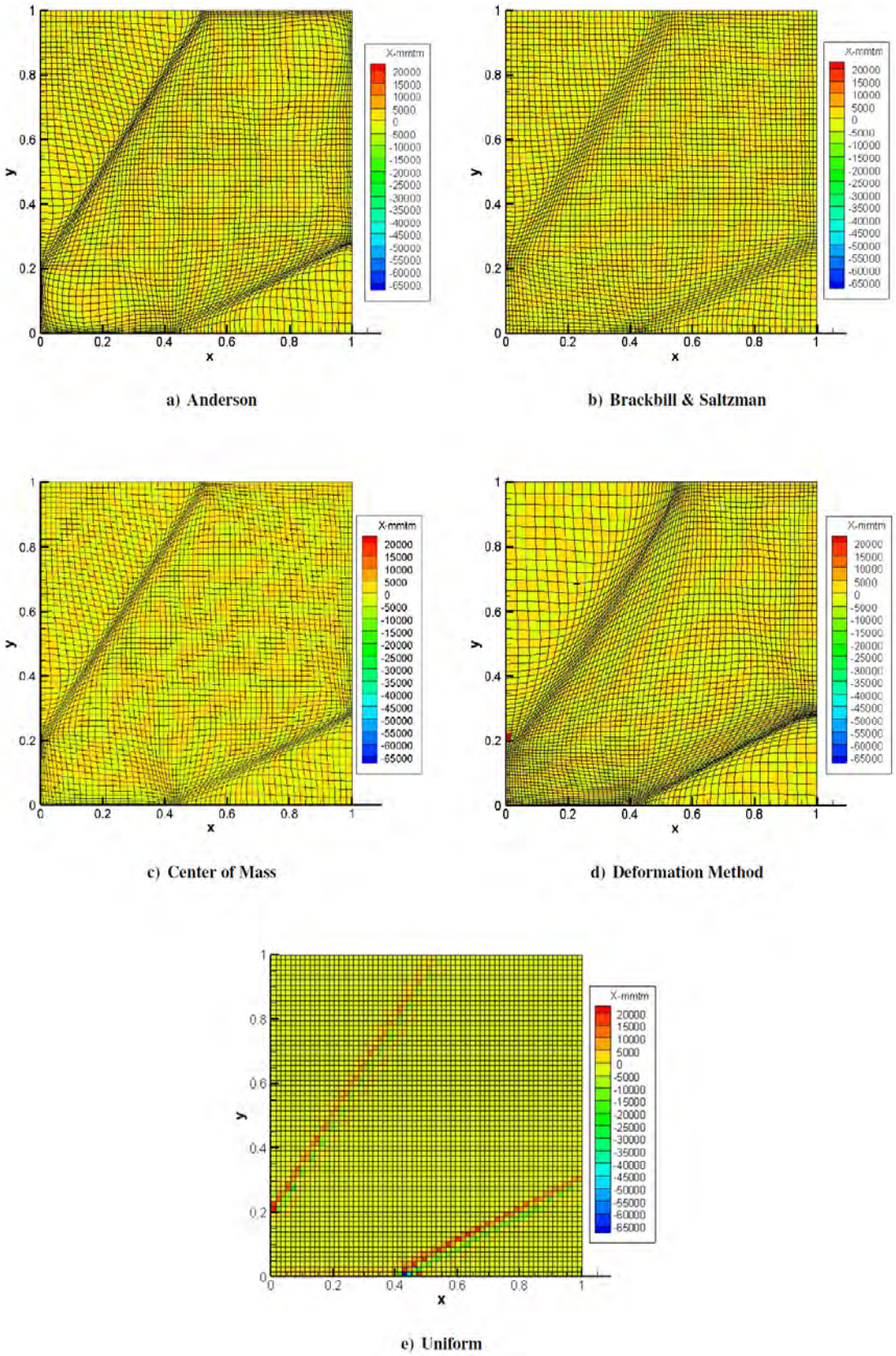

Figure 22. Truncation error for the x-momentum equation: edge case.

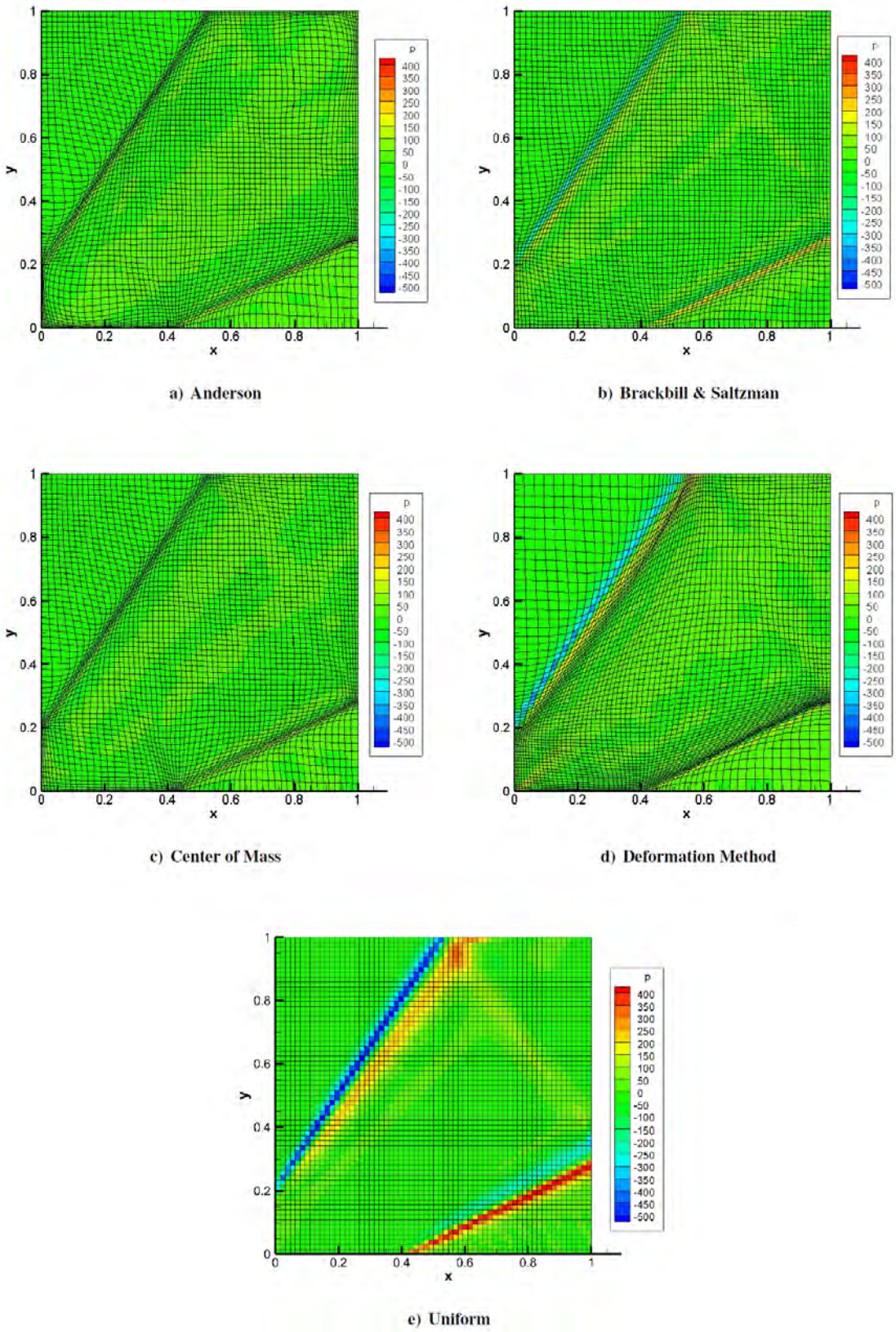

Figure 23. Discretization error for the pressure: edge case.

Discretization error comparisons for u-velocity along a line through the domain at $x = 0.5$ m is shown in Figure 24. The spikes in discretization error in this figure at approximately $y = 0.05$ m and y = 0.95 m correspond to the edges of the expansion fan. It can be seen that the Anderson and center of mass adaptation schemes best reduce these spikes in discretization error. Figure 25 illustrates the adaptive convergence of the Anderson adaptation scheme for this case. The L_2 norm of truncation error and the weight function equidistribution error are plotted against the number of adaptation cycles. Although it may appear that these monitors could converge further, truncation error norms do not continue to converge and no increased benefit is found by adapting more than 50 adaptation cycles for this case.

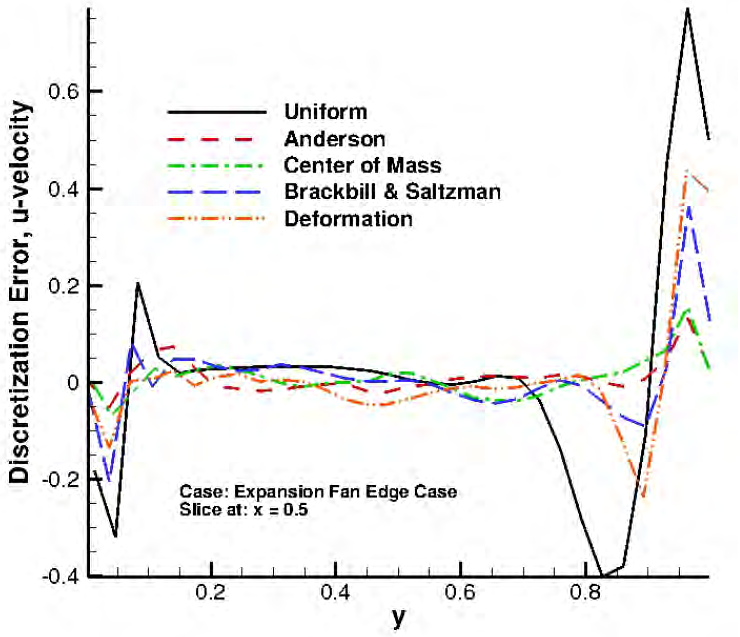

Figure 24. Discretization error for *u*-velocity at $x = 0.5$ m: edge case.

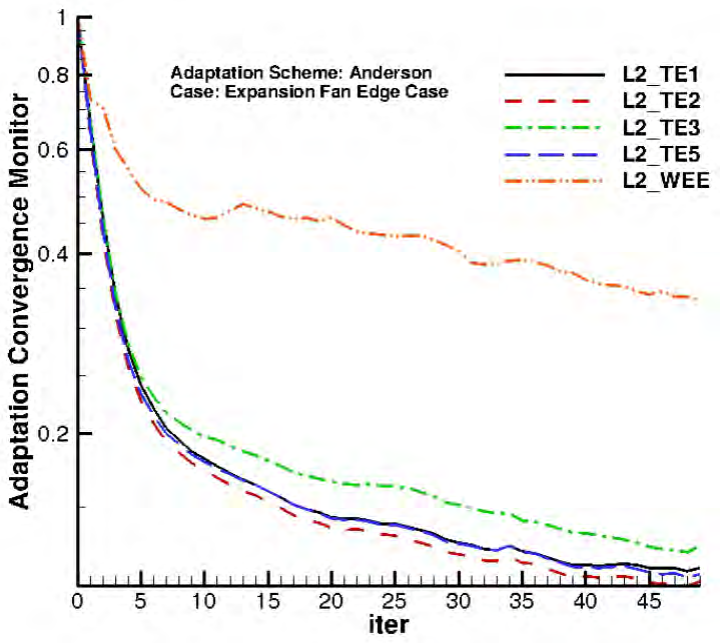

Figure 25. Adaptive convergence: Anderson method (edge case).

Corner Case

Truncation and discretization error improvements for the corner case of the supersonic expansion fan achieved by each adaptation scheme may be found in Tyson et al. (2015). Similar to the edge case, the greatest truncation error reduction is achieved using the center of mass approach with about an eight time reduction. Discretization error for this adaptation scheme is reduced by a factor of approximately five for each primitive variable. Although Anderson's adaptation scheme does not perform as well here as with the edge case, over a three time improvement in discretization error is achieved. The Brackbill and Saltzman and Deformation adaptation schemes achieve a peak reduction factor in discretization error of 1.87 and 1.49, respectively.

Most of the discretization error for this case is present in the bottom left corner of the domain at the start of the expansion fan. With this in mind, discretization error is only plotted for each adaptation scheme in the bottom left corner of the domain to better illustrate the results for each adaptation method. Discretization error in density is given in Figure 26. It can be seen in Figure 26a and Figure 26c how well the Anderson and center of mass schemes reduce discretization error in this region relative to the Brackbill and Saltzman and Deformation adaptation schemes, Figure 26b and Figure 26d, respectively.

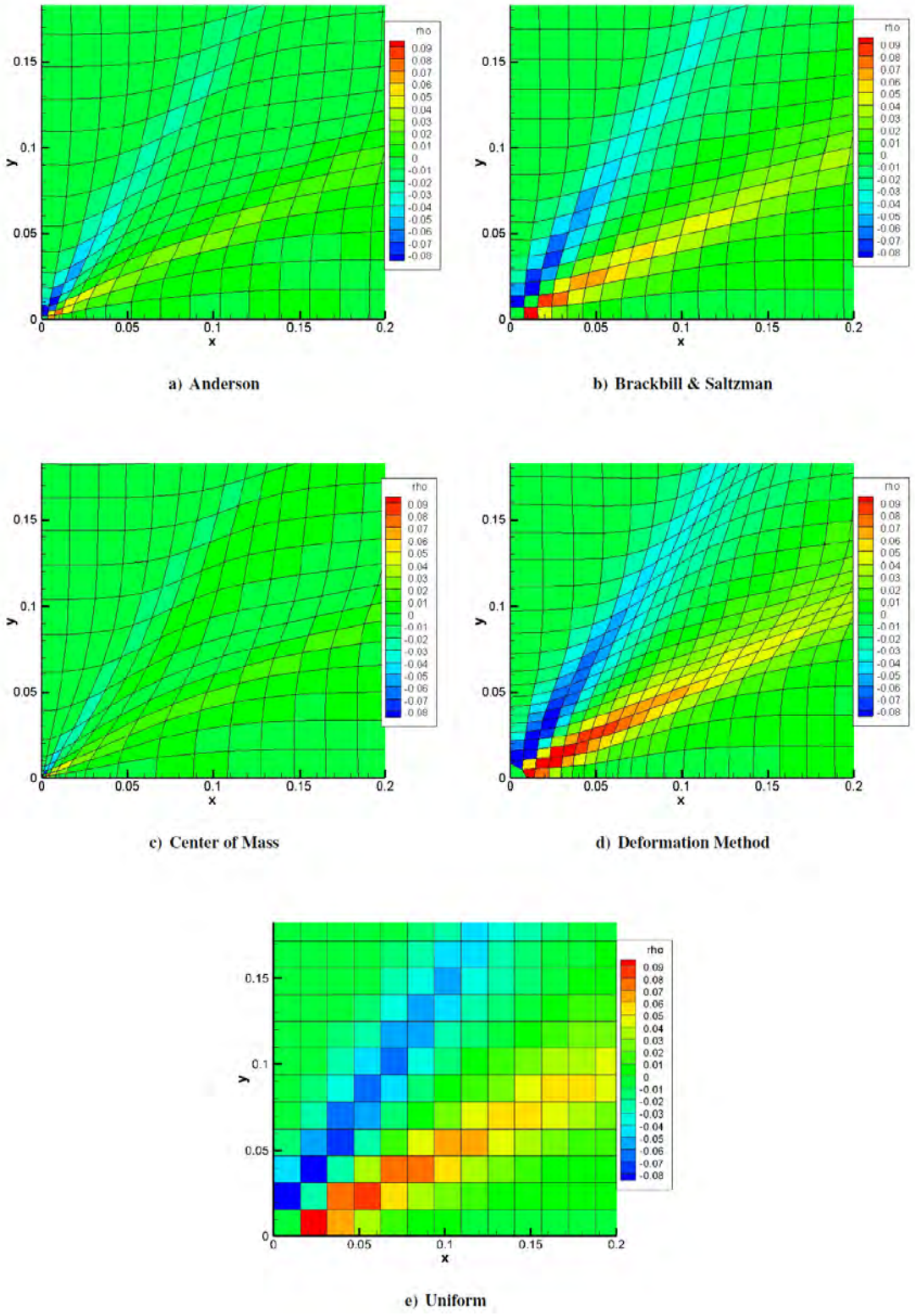

a) Anderson

b) Brackbill & Saltzman

c) Center of Mass

d) Deformation Method

e) Uniform

Figure 26. Discretization error for the density: corner case.

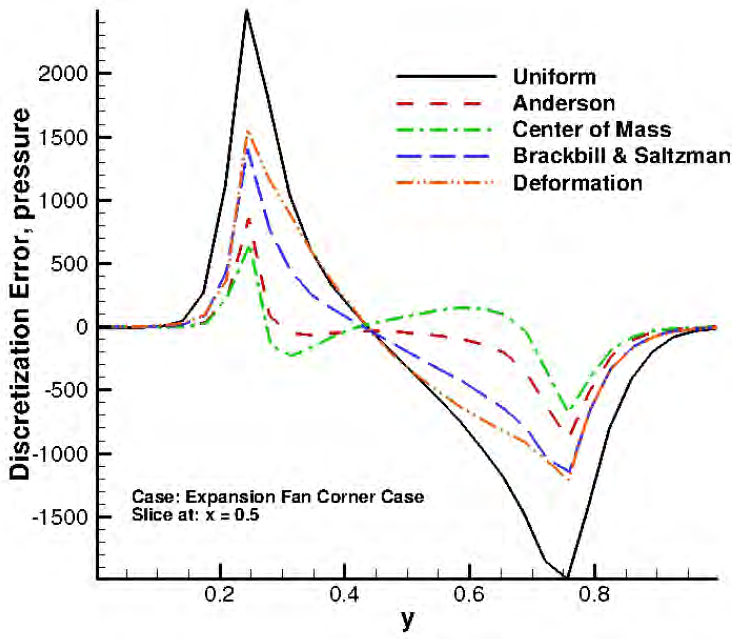

Figure 27. Discretization error for pressure at x = 0.5 m: corner case.

Figure 10. Discretization Error in Pressure at x = 0.5m

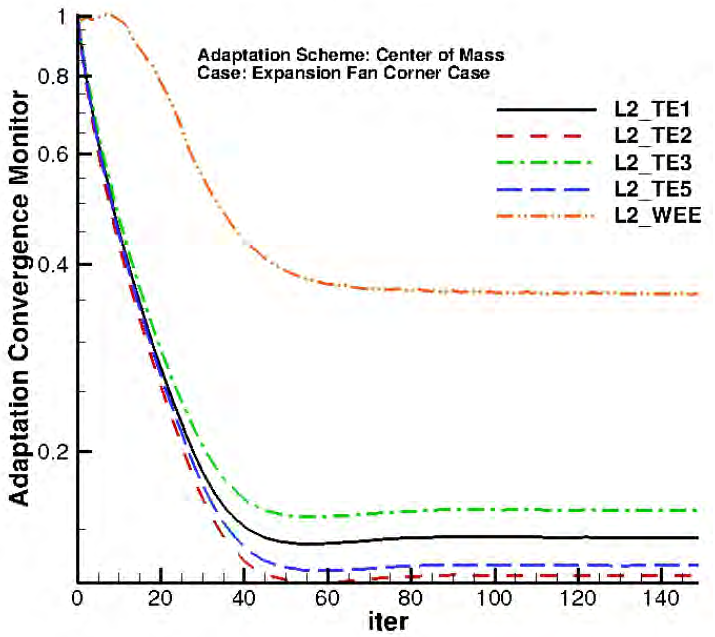

Figure 28. Adaptive convergence: center of mass method (corner case).

Figure 11. Adaptive Convergence: Center of Mass

Discretization error comparisons for pressure along a line through the domain at x = 0.5m may be found in Figure 27. Similar to the edge case, the spikes in discretization error in this figure at approximately y = 0.25m and y = 0.75m correspond to the edges of the expansion fan. Again, the Anderson and center of mass adaptation schemes are able to reduce these spikes in discretization error the most. Figure 28 illustrates the adaptive convergence of the center of mass adaptation scheme for this case. The L_2 norm of truncation error and the weight function equidistribution error are plotted against the number of adaptation cycles. Here adaptation is performed for 150 adaptation cycles. Past 50 adaptation cycles, the adaptation is converged and no added benefit is achieved by further adaptation.

Shifted Case

The discretization error in pressure for the shifted case is shown in Figure 29 for the uniform mesh and the center of mass adaptation method. The center of mass approach achieved a factor of 13.5 reduction in the L_2 norm of the discretization error in the pressure. These higher improvement factors relative to the corner case are due to the singularity being located on only one boundary instead of the intersection of two boundaries. The discretization error in the pressure extracted from a line at x = 0.5 m is shown in Figure 30. Large reductions in the error are found at the beginning and ending of the expansion fan relative to the uniform mesh.

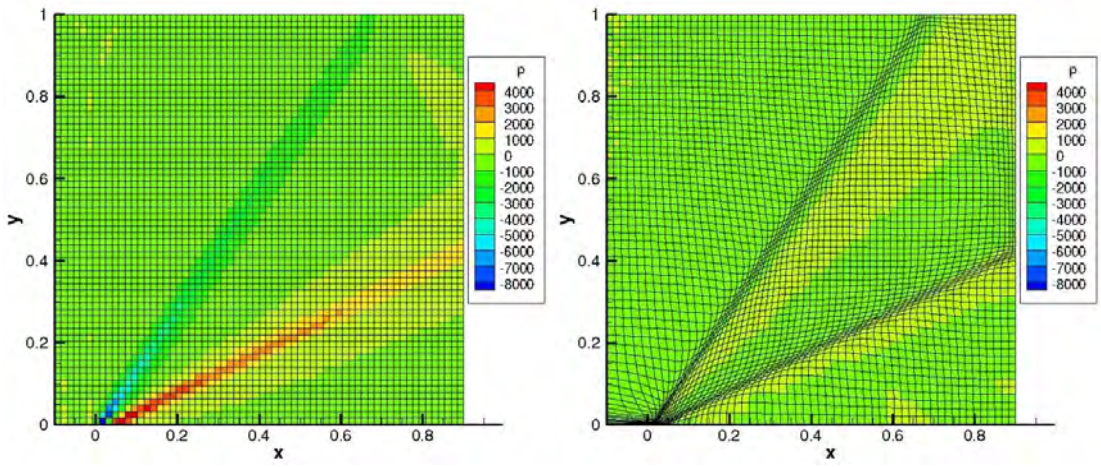

Figure 29. Discretization error in pressure for the shifted case: uniform mesh (left) and center of mass adapted mesh (right).

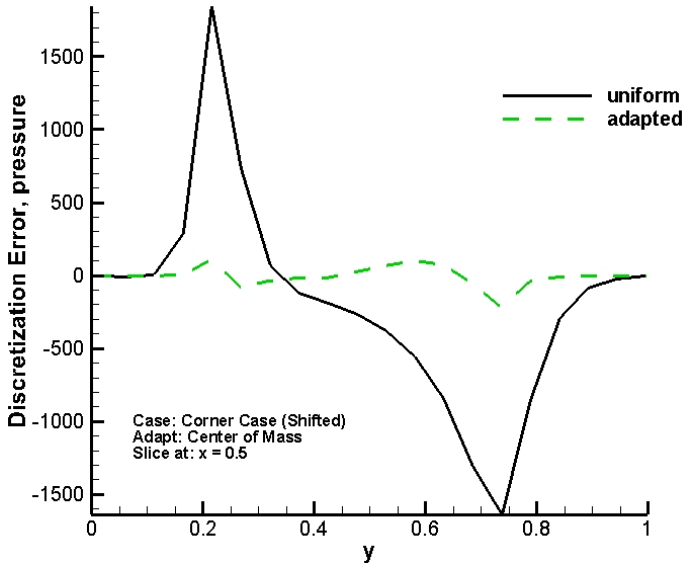

Figure 30. Discretization error for pressure at $x = 0.5$ m: shifted case.

Grid Study

A grid study is conducted for the corner case of the 2D expansion fan. The L_2 norm of discretization error in pressure is compared on uniform and adapted grids for five uniformly refined grid levels ranging from 9×9 to 129×129. Each adapted grid in this study is generated independently starting from a uniform grid. Figure 31 illustrates the savings which can be achieved when using r-adaptation as a means of reducing discretization error. For example, to achieve the same level of discretization error as the coarsest adapted grid, a uniform grid which is three grid levels finer would be required. This uniform grid would have 64 times the number of cells of the coarsest adapted grid for this 2D problem. It would be 512 times as many cells in 3D. This equates to huge computational savings especially when a lower level of discretization error is desired. Similar trends can also be seen with the other primitive variables for this case. Also, the order of convergence between the uniform and adapted grids is quite similar. This is surprising considering the adaptation schemes used in this study provide no guarantee that the order of convergence on adapted grids will be the same as consistently refined unadapted grids. The order of convergence using discretization error in pressure for the three finest grid levels is computed to be $\hat{p} = 0.68$. This convergence rate is consistent with what is expected for problems containing linear discontinuities such as this expansion fan case. Banks et al. (2008) show that for problems with linear discontinuities the observed order of accuracy will reduce to:

$$\hat{p} = \frac{p_f}{p_f + 1} \tag{71}$$

where p_f is the formal order of accuracy of the discretization. With a formal order of accuracy of $p_f = 2$, the expected order of accuracy for this case will be $\hat{p} = 0.66$.

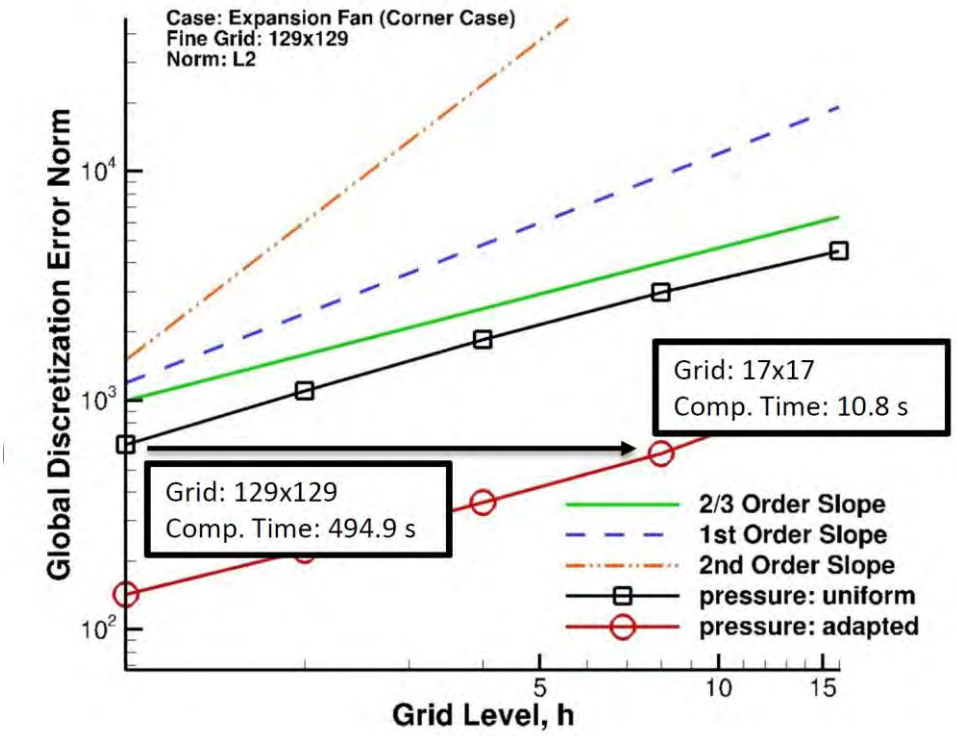

Figure 31. Grid study showing the behavior of the L_2 norm of discretization error in pressure for uniform and center of mass adapted meshes: corner case.

XI. Publications Supported in Whole or in Part by this Grant

1. T. S. Phillips, J. M. Derlaga, C. J. Roy, and J. Borggaard, "Finite Volume Solution Reconstruction Methods for Truncation Error Estimation," manuscript submitted to the *Journal of Computational Physics*, October 2014.
2. J. M. Derlaga, T. S. Phillips, and C. J. Roy, "SENSEI Computational Fluid Dynamics Code: A Case Study in Modern Fortran Software Development," manuscript submitted to *Computers and Fluids*, February 2015.
3. J. M. Derlaga, C. J. Roy, and J. Borggaard, "Adjoint and Truncation Error Based Adaptation for 1D Finite Volume Schemes," manuscript submitted to the *Journal of Computational Physics*, May 2015.
4. T. S. Phillips, C. J. Roy, and J. Borggaard, "Residual-Based Discretization Error Estimators for the Euler and Navier-Stokes Equations," manuscript submitted to the *Journal of Computational Physics*, May 2015.
5. T. S. Phillips, J. M. Derlaga, and C. J. Roy, "Numerical Benchmark Solutions for Laminar and Turbulent Flows," AIAA Paper 2012-3074, 42nd AIAA Fluid Dynamics Conference and Exhibit, 25 - 28 June 2012, New Orleans, Louisiana.
6. T. S. Phillips, C. J. Roy, E. J. Alyanak, and C. F. Ollivier-Gooch, "Optimal Mesh Adaption for Burgers' Equation," AIAA Paper 2012-2710, 42nd AIAA Fluid Dynamics Conference and Exhibit, 25 - 28 June 2012, New Orleans, Louisiana.
7. C. F. Ollivier-Gooch and C. J. Roy, "Reducing Truncation Error on Unstructured Meshes by Vertex Movement," AIAA Paper 2012-2712, 42nd AIAA Fluid Dynamics Conference and Exhibit, 25 - 28 June 2012, New Orleans, Louisiana.

8. J. M. Derlaga, T. S. Phillips, and C. J. Roy, "SENSEI Computational Fluid Dynamics Code: A Case Study in Modern Fortran Software Development," AIAA Paper 2013-2450, 21st AIAA Computational Fluid Dynamics Conference, San Diego, CA, June 24-27, 2013.
9. J. M. Derlaga, C. J. Roy, and J. Borggaard, "Adjoint and Truncation Error Based Adaptation for 1D Finite Volume Schemes," AIAA Paper 2013-2865, 21st AIAA Computational Fluid Dynamics Conference, San Diego, CA, June 24-27, 2013.
10. T. S. Phillips, J. M. Derlaga, C. J. Roy, and J. Borggaard, "Finite Volume Solution Reconstruction Methods for Truncation Error Estimation," AIAA Paper 2013-3090, 21st AIAA Computational Fluid Dynamics Conference, San Diego, CA, June 24-27, 2013.
11. T. S. Phillips, C. J. Roy, and J. Borggaard, "Error Transport Equation Boundary Conditions for the Euler and Navier-Stokes Equations," AIAA Paper 2014-1432, 52nd Aerospace Sciences Meeting, National Harbor, MD, January 13-17, 2014.
12. T. S. Phillips and C. J. Roy, "Defect Correction and Error Transport Discretization Error Estimation for Applications in CFD," AIAA Paper 2014-2572, 32nd AIAA Applied Aerodynamics Conference, AIAA Aviation and Aeronautics Forum and Exposition 2014, Atlanta, GA, June 16-20, 2014.
13. J. Derlaga, T. Phillips, C. J. Roy, and J. Borggaard, "Adjoint and Truncation Error Based Adaptation for Finite Volume Schemes with Error Estimates," AIAA Paper 2015-1262, 53rd AIAA Aerospace Sciences Meeting, 5 - 9 January 2015, Kissimmee, Florida.
14. W. C. Tyson, J. M. Derlaga, C. J. Roy, and A. Choudhary, "Comparison of r-Adaptation Techniques for 2-D CFD Applications," AIAA Paper 2015-2611, 22nd AIAA Computational Fluid Dynamics Conference, June 22-26, 2015, Dallas, Texas.

XII. Theses Supported by this Grant

1. Tyrone S. Phillips, "Residual-based Discretization Error Estimation for Computational Fluid Dynamics," PhD Thesis, Virginia Polytechnic Institute and State University, September 2014
2. Joseph M. Derlaga, "Application of Improved Truncation Error Estimation Techniques to Adjoint Based Error Estimation and Grid Adaptation," PhD Thesis, Virginia Polytechnic Institute and State University, July 2015.

XIII. References

Ainsworth, M. and Oden, J.T. (2000). *A Posteriori Error Estimation in Finite Element Analysis*, Wiley Interscience, New York.

Alyanak, E.J., Roy, C.J., and Choudhary, A. (2011). "Investigation of Optimal Grid Distributions for Burgers Equation," AIAA Paper 2011-888, AIAA Aerospace Sciences Meeting, Orlando, FL, January 2011.

Anderson, D., "Grid Cell Volume Control with an Adaptive Grid Generator," Applied Mathematics and Computation, Vol. 35, 1990, pp. 209 – 217.

Baker, T.J. (1997). "Mesh Adaptation Strategies for Problems in Fluid Dynamics," *Finite Elements in Analysis and Design*, Vol. 25, pp. 243-273.

Banks, J., Aslam, T., and Rider,W., "On sub-linear convergence for linearly degenerate waves in capturing schemes," *Journal of Computational Physics*, Vol. 227, No. 14, 2008, pp. 6985 – 7002.

Barth, T. J., "Higher order solution of the euler equations on unstructured grids using quadratic reconstruction," Tech. Rep. AIAA-90-0013, 1990. Initial development of K-exact method.

Barth, T. J., "Recent developments in higher order k-exact reconstruction on unstructured meshes," Tech. Rep. AIAA-93-0668, 1993.

Bernert, K. (1997). "τ-Extrapolation – Theoretical Foundation, Numerical Experiment, and Application to Navier-Stokes Equations," *SIAM Journal of Scientific Computing*, Vol. 18, No. 2, pp. 460-478.

Brackbill, J.U. and Saltzman, J.S. (1982). "Adaptive Zoning for Singular Problems in 2 Dimensions," *Journal of Computational Physics*, Vol. 46, No. 3, pp. 342-368.

Burkardt, J. "Clenshaw curtis quadrature rules." http://people.sc.fsu.edu/˜jburkardt/m_src/ccn_rule/ccn_rule.html, 2010.

Cavallo, P.A. and Sinha, N. (2007). "Error Quantification for Computational Aerodynamics Using an Error Transport Equation," *Journal of Aircraft*, Vol. 44, No. 6, pp. 1954-1963.

Choudhary, A., "Verification of Compressible and Incompressible Computational Fluid Dynamics Codes and Residual-based Mesh Adaptation," Ph.D. thesis, Virginia Polytechnic Institute and State University, Blacksburg, VA, 2014.

Choudhary, A. and Roy, C.J. (2011). "Efficient Residual-Based Mesh Adaptation for 1D and 2D CFD Applications," AIAA Paper 2011-214.

Clenshaw, C. W. and A. R. Curtis, "A method for numerical integration on an automatic computer," Numerische Mathematik, vol. 2, pp. 197–205, 1960. http://www.digizeitschriften.de/dms/img/?PPN=GDZPPN001163442.

Derlaga, J. M., T. S. Phillips, and C. J. Roy, "SENSEI Computational Fluid Dynamics Code: A Case Study in Modern Fortran Software Development," AIAA Paper 2013-2450, 21st AIAA Computational Fluid Dynamics Conference, San Diego, CA, June 24-27, 2013.

Diskin, B. and J. L. Thomas (2007). Accuracy Analysis for Mixed-Element Finite Volume Discretization Schemes, Technical Report TR 2007–8, Hampton, VA, National Institute of Aerospace.

Dwight, R.P. (2008). "Heuristic A Posteriori Estimation of Error due to Dissipation in Finite Volume Schemes and Application to Mesh Adaptation," *Journal of Computational Physics*, Vol. 227, No. 5, pp. 2845-2863.

Fidkowski, K.J. and Darmofal, D.L. (2011). "Review of Output-Based Error Estimation and Mesh Adaptation in Computational Fluid Dynamics," *AIAA Journal*, Vol. 49, No. 4, pp. 673-694.

Fraysse, F., J. de Vicente, and E. Valero, "The estimation of truncation error by t-estimation revisited," *Journal of Computational Physics*, vol. 231, pp. 3457–3482, 2012.

Fulton, S. R., "On the accuracy of multigrid truncation error estimates," Electronic Transactions on Numerical Analysis, vol. 15, pp. 29–37, 2003.

Garbey, M. and Shyy, W. (2003). "A Least Square Extrapolation Method for Improving Solution Accuracy of PDE Computations," *Journal of Computational Physics*, Vol. 186, No. 1, pp. 1–23.

Giles, M. and Pierce, N., "An Introduction to the Adjoint Approach to Design," *Flow, Turbulence and Combustion*, Vol. 65, 2000, pp. 393-415.

Godfrey, A. G., C. R. Mitchell, and R. W. Walters, "Practical aspects of spatially high-order accurate methods," AIAA Journal, vol. 31, no. 9, pp. 1634–1642, 1993.

Gu, X. and T.I-P. Shih (2001). "Differentiating between Source and Location of Error for Solution-Adaptive Mesh Refinement," AIAA Paper 2001–2660.

Harten, A. and S. Osher, "Uniformly high-order accurate nonoscillatory schemes i," SIAM Journal of Numerical Analysis, vol. 24, pp. 279–309, 1987. First development of ENO scheme-1D.

Hesthaven, J.S. and Warburton, T. (2008). *Nodal Discontinuous Galerkin Methods: Algorithms, Analysis, and Applications*, Texts in Applied Mathematics, Vol. 54, Springer, New York (DOI: 10.1007/978-0-387-72067-8).

Hirsch, C. (1988). *Numerical Computation of Internal and External Flows, Vol. 2: Computational Methods for Inviscid and Viscous Flows*, John Wiley & Sons, New York.

Laflin, K., Solver-Independent r-Refinement Adaptation for Dynamic Numerical Simulations, Ph.D. thesis, North Carolina State University, 1997

Lapenta, G. (2003). "Variational Grid Adaptation Based on the Minimization of Local Truncation Error: Time-Independent Problems," *Journal of Computational Physics*, Vol. 193, pp. 159-179.

Layton, W., Lee, H.K., and Peterson, J. (2002). "A Defect-Correction Method for the Incompressible Navier-Stokes Equations," *Applied Mathematics and Computation*, Vol. 129, pp. 1-19.

Lee, D. and Tsuei, Y.M. (1992). "A Formula for Estimation of Truncation Errors of Convective Terms in a Curvilinear Coordinate System," *Journal of Computational Physics*, Vol. 98, pp. 90-100.

Liao, G. and Anderson, D., "A New Approach to Grid Generatino," Applicable Analysis, Vol. 44, No. 3-4, 1992, pp. 285-298.

Love, M.H., Yoakum, R.E., and Britt, R.T. (2003). "Identification of Critical Flight Loads," AIAA Paper 2003-1893, 44th AIAA/ASME/ASCE/AHS/ASC Structures, Structural Dynamics, and Materials Conference, April 7-10, 2003.

Mastin, C.W. (1999). "Truncation Error on Structured Grids," in *Handbook of Grid Generation*, J. F. Thompson, B. K. Soni, and N. P. Weatherill, Eds., CRC Press, Boca Raton.

McRae, D.S. (2000). "r-refinement Grid Adaptation Algorithms and Issues," *Computer Methods in Applied Mechanics and Engineering*, Vol. 189, pp. 1161–1182.

Morrison, J.H. and Hemsch, M.J. (2007). "Statistical Analysis of CFD Solutions from the Third AIAA Drag Prediction Workshop (Invited)," AIAA Paper 2007-254, 45th AIAA Aerospace Sciences Meeting and Exhibit, 8 - 11 January 2007, Reno, Nevada.

Nakahashi, K. and Deiwert, G.S. (1986). "Three-Dimensional Adaptive Grid Method," *AIAA Journal*, Vol. 24, pp. 948-954.

Naumovich, A., Forster, M., and Dwight, R. (2010). "Algebraic Multigrid within Defect Correction for the Linearized Euler Equations," *Numerical Linear Algebra with Applications*, Vol. 17, pp. 307-324.

Nemec, M. and Aftosmis, M. J., "Adjoint Error Estimation and Adaptive Refinement for Embedded-Boundary Cartesian Meshes," AIAA Paper 2007-4187, 18th AIAA Computational Fluid Dynamics Conference, Miami, Florida, June 25-28, 2007.

Oberkampf, W.L. and Roy, C.J. (2010). *Verification and Validation in Scientific Computing*, Cambridge University Press, Cambridge.

Pereyra, V., "On improving an approximate solution of a functional by deferred corrections," Numerische Mathematik, vol. 8, pp. 376–391, 1965.

Pereyra, V., "Iterated Deferred Corrections for Nonlinear Operator Equations," Numerische Mathematik, Vol. 10, No. 4, 1967, pp. 316-323.

Pereyra, V., "Iterated Deferred Corrections for Nonlinear Boundary Value Problems," Numerische Mathematik, Vol. 11, No. 2, 1968, pp. 111-125.

Phillips, T.S. and Roy, C.J. (2011). "Residual Methods for Discretization Error Estimation," paper accepted for presentation at the 20th AIAA CFD Conference, Honolulu, Hawaii, June 2011.

Phillips, T. S. and C. J. Roy, "A new extrapolation-based uncertainty estimator for computational fluid dynamics," AIAA-2013-0260, 2013.

Pierce, N.A. and Giles, M.B. (2000). "Adjoint Recovery of Superconvergent Functionals from PDE Approximations," *SIAM Review*, Vol. 42, No. 2, pp. 247–264.

Qin, Y., and T. I.-P. Shih, "A discrete transport equation for error estimation in cfd," Tech. Rep. AIAA-2002-0906, 2002.

Roache, P.J. (2009). *Fundamentals of Verification and Validation*, Hermosa Publishers, Socorro, New Mexico.

Roe, P.J. (1981). "Approximate Riemann Solvers, Parameter Vectors, and Difference Schemes," *Journal of Computational Physics*, Vol. 43, No. 2, pp. 357–372.

Roy, C.J. (2005). "Review of Code and Solution Verification Procedures for Computational Simulation," *Journal of Computational Physics*, Vol. 205, No. 1, pp. 131-156

Roy, C.J. (2009). "Strategies for Driving Mesh Adaptation in CFD (Invited)," AIAA Paper 2009-1302, 47th AIAA Aerospace Sciences Meeting, 5 - 8 January 2009, Orlando, Florida.

Roy, C.J. (2010a). "Review of Discretization Error Estimators in Scientific Computing," AIAA Paper 2010-126, 48th AIAA Aerospace Sciences Meeting, 4 - 7 January 2010, Orlando, Florida.

Roy, C.J. (2010b). "Survey of Residual-based Methods for Estimating Discretization Error," American Nuclear Society: 2010 Winter Meeting and Nuclear Technology Expo, Las Vegas, Nevada.

Roy, C.J. and Oberkampf, W.L. (2011). "A Comprehensive Framework for Verification, Validation, and Uncertainty Quantification in Scientific Computing," *Computer Methods in Applied Mechanics and Engineering*, Vol. 200, Nos. 25-28, pp. 2131-2144 (DOI: 10.1016/j.cma.2011.03.016).

Rumsey, C.L., Smith, B.R., and Huang, G.P. (2010). "Description of a Website Resource for Turbulence Model Verification and Validation," AIAA Paper 2010-4742, 40th AIAA Fluid Dynamics Conference, June 28 - July 1, 2010, Chicago, Illinois (see http://turbmodels.larc.nasa.gov/).

Shih, T.I-P. and Williams, B.R. (2009). "Development and Evaluation of an a posteriori Method for Estimating and Correcting Grid-induced Errors in Solutions of the Navier-Stokes Equations," AIAA Paper 2009-1499.

Skeel, R.D. (1986). "Thirteen Ways to Estimate Global Error," *Numerische Mathematik*, Vol. 48, pp. 1-20.

Smolyak, S. A., "Quadrature and interpolation formulas for tensor products of certain classes of functions," Dok. Akad. Nauk SSSR, vol. 4, pp. 240–243, 1963. Found reference: Gerstner and Briebel, Numerical Algorithms 18 (1998) 209-232.

Squire, W. and Trapp, G. (1998). "Using Complex Variables to Estimate Derivatives of Real Functions," *SIAM Review*, Vol. 40, No. 1, pp. 110-112.

Stetter, H.J. (1978). "The Defect Correction Principle and Discretization Methods," *Numerische Mathematik*, Vol. 29, pp. 425-443.

Syrakos, A. and Goulas, A. (2006). "Estimate of the Truncation Error of Finite Volume Discretization of the Navier-Stokes Equations on Colocated Grids," *International Journal for Numerical Methods in Fluids*, Vol. 50, pp. 103-130.

Thompson, J.F., Warsi, Z.U.A., and Mastin, C.W. (1985). *Numerical Grid Generation: Foundations and Applications*, Elsevier, New York.

Tyson, W. C., J. M. Derlaga, C. J. Roy, and A. Choudhary, "Comparison of r-Adaptation Techniques for 2-D CFD Applications," AIAA Paper 2015-2611, 22nd AIAA Computational Fluid Dynamics Conference, June 22-26, 2015, Dallas, Texas

van Albada, G., van Leer, B., and Roberts, W. J., "A comparative study of computational methods in cosmic gas dynamics," *Astronomy and Astrophysics*, Vol. 108, No. 1, 1982, pp. 76-84.

van Leer, B., "Towards the Ultimate Conservative Difference Scheme. V. A Second-order Sequel to Godunov's Method," *Journal of Computational Physics*, Vol. 32, No. 1, 1979, pp. 101-136.

Venditti, D.A. and Darmofal, D.L. (2003). "Anisotropic Grid Adaptation for Functional Outputs: Application to Two-Dimensional Viscous Flows," *Journal of Computational Physics*, Vol. 187, pp. 22–46.

Wang, L. and Mavriplis, D.J. (2009). "Adjoint-based h–p Adaptive Discontinuous Galerkin Methods for the 2D Compressible Euler Equations," *Journal of Computational Physics*, Vol. 228, No. 20, pp. 7643-7661.

Yamaleev, N.K. (2001). "Minimization of the Truncation Error by Grid Adaptation," *Journal of Computational Physics*, Vol. 170, pp. 459-497.

Yamaleev, N. K., Diskin, B. and Pathakz, K. (2010). "Error Minimization via Adjoint-Based Anisotropic Grid Adaptation," AIAA Paper 2010-4436, 40th Fluid Dynamics Conference, 28 June - 1 July 2010, Chicago, Illinois.

Zadunaisky, P.E. (1966). "A Method for the Estimation of Errors Propagated in the Numerical Solution of a System of Ordinary Differential Equations," in *Proceedings of the Astronautical Union*, Symposium No. 25, New York, Academic Press.

Zienkiewicz, O.C. and Zhu, J Z. (1992). "The Superconvergent Patch Recovery and *A Posteriori* Error Estimates, Part 2: Error Estimates and Adaptivity," *International Journal for Numerical Methods in Engineering*, Vol. 33, pp. 1365-1382.

Zhang, X. D., D. Pelletier, and J.-Y. Trepanier, "Verification of error estimators for the Euler equations," Tech. Rep. AIAA-2000-1001, 2000.

1.

1. Report Type

Final Report

Primary Contact E-mail
Contact email if there is a problem with the report.

cjroy@vt.edu

Primary Contact Phone Number
Contact phone number if there is a problem with the report

540-231-0080

Organization / Institution name

Virginia Tech

Grant/Contract Title
The full title of the funded effort.

Residual-based Methods for Controlling Discretization Error in CFD

Grant/Contract Number
AFOSR assigned control number. It must begin with "FA9550" or "F49620" or "FA2386".

FA9550-12-1-0173

Principal Investigator Name
The full name of the principal investigator on the grant or contract.

Christopher John Roy

Program Manager
The AFOSR Program Manager currently assigned to the award

Jean-Luc Cambier

Reporting Period Start Date

05/01/2012

Reporting Period End Date

04/30/2015

Abstract

Computational Fluid Dynamics (CFD) has enormous potential to impact the analysis, design, and optimization of U.S. Air Force flight systems. The objective of our work is to develop and demonstrate methods for the reliable and automatic control of discretization error in CFD. Our approach will provide designers and analysts with techniques to quantify and reduce discretization error in CFD predictions without the overhead of creating, and solving on, multiple meshes. Our work will lead to significant improvements in the accuracy and efficiency of CFD predictions of aerodynamic loads. We will investigate the following residual-based discretization error estimation techniques unified within the PI's generalized truncation error estimation framework: discretization error transport equations, defect correction methods, and adjoint methods. We will also develop mesh adaptation techniques wherein the mesh is automatically adapted to reduce discretization error in the solution or solution functionals (i.e., aerodynamic loads). The adaptation will be driven by the residuals/truncation errors, which serve as the local source of discretization error, rather than ad hoc solution features (e.g., gradients, shock waves).

Distribution Statement
This is block 12 on the SF298 form.

Distribution A - Approved for Public Release

Explanation for Distribution Statement

If this is not approved for public release, please provide a short explanation. E.g., contains proprietary information.

SF298 Form

Please attach your SF298 form. A blank SF298 can be found here. Please do not password protect or secure the PDF The maximum file size for an SF298 is 50MB.

SF298-AFOSR-Roy.pdf

Upload the Report Document. File must be a PDF. Please do not password protect or secure the PDF . The maximum file size for the Report Document is 50MB.

AFOSR-Residuals-Final-Report.final.pdf

Upload a Report Document, if any. The maximum file size for the Report Document is 50MB.

Archival Publications (published) during reporting period:

1. T. S. Phillips, J. M. Derlaga, and C. J. Roy, "Numerical Benchmark Solutions for Laminar and Turbulent Flows," AIAA Paper 2012-3074, 42nd AIAA Fluid Dynamics Conference and Exhibit, 25 - 28 June 2012, New Orleans, Louisiana.
2. T. S. Phillips, C. J. Roy, E. J. Alyanak, and C. F. Ollivier-Gooch, "Optimal Mesh Adaption for Burgers' Equation," AIAA Paper 2012-2710, 42nd AIAA Fluid Dynamics Conference and Exhibit, 25 - 28 June 2012, New Orleans, Louisiana.
3. C. F. Ollivier-Gooch and C. J. Roy, "Reducing Truncation Error on Unstructured Meshes by Vertex Movement," AIAA Paper 2012-2712, 42nd AIAA Fluid Dynamics Conference and Exhibit, 25 - 28 June 2012, New Orleans, Louisiana.
4. J. M. Derlaga, T. S. Phillips, and C. J. Roy, "SENSEI Computational Fluid Dynamics Code: A Case Study in Modern Fortran Software Development," AIAA Paper 2013-2450, 21st AIAA Computational Fluid Dynamics Conference, San Diego, CA, June 24-27, 2013.
5. J. M. Derlaga, C. J. Roy, and J. Borggaard, "Adjoint and Truncation Error Based Adaptation for 1D Finite Volume Schemes," AIAA Paper 2013-2865, 21st AIAA Computational Fluid Dynamics Conference, San Diego, CA, June 24-27, 2013.
6. T. S. Phillips, J. M. Derlaga, C. J. Roy, and J. Borggaard, "Finite Volume Solution Reconstruction Methods for Truncation Error Estimation," AIAA Paper 2013-3090, 21st AIAA Computational Fluid Dynamics Conference, San Diego, CA, June 24-27, 2013.
7. T. S. Phillips, C. J. Roy, and J. Borggaard, "Error Transport Equation Boundary Conditions for the Euler and Navier-Stokes Equations," AIAA Paper 2014-1432, 52nd Aerospace Sciences Meeting, National Harbor, MD, January 13-17, 2014.
8. T. S. Phillips and C. J. Roy, "Defect Correction and Error Transport Discretization Error Estimation for Applications in CFD," AIAA Paper 2014-2572, 32nd AIAA Applied Aerodynamics Conference, AIAA Aviation and Aeronautics Forum and Exposition 2014, Atlanta, GA, June 16-20, 2014.
9. J. Derlaga, T. Phillips, C. J. Roy, and J. Borggaard, "Adjoint and Truncation Error Based Adaptation for Finite Volume Schemes with Error Estimates," AIAA Paper 2015-1262, 53rd AIAA Aerospace Sciences Meeting, 5 - 9 January 2015, Kissimmee, Florida.
10. W. C. Tyson, J. M. Derlaga, C. J. Roy, and A. Choudhary, "Comparison of r-Adaptation Techniques for 2-D CFD Applications," AIAA Paper 2015-2611, 22nd AIAA Computational Fluid Dynamics Conference, June 22-26, 2015, Dallas, Texas.
11. Tyrone S. Phillips, "Residual-based Discretization Error Estimation for Computational Fluid Dynamics," PhD Thesis, Virginia Polytechnic Institute and State University, September 2014
12. Joseph M. Derlaga, "Application of Improved Truncation Error Estimation Techniques to Adjoint Based Error Estimation and Grid Adaptation," PhD Thesis, Virginia Polytechnic Institute and State University, July 2015.

Changes in research objectives (if any):

None

Change in AFOSR Program Manager, if any:

Fariba Fahroo was initial program manager. Jean-Luc Cambier is the new program manager (effective

after the grant ended).

Extensions granted or milestones slipped, if any:

None

AFOSR LRIR Number

LRIR Title

Reporting Period

Laboratory Task Manager

Program Officer

Research Objectives

Technical Summary

Funding Summary by Cost Category (by FY, $K)

	Starting FY	FY+1	FY+2
Salary			
Equipment/Facilities			
Supplies			
Total			

Report Document

Report Document - Text Analysis

Report Document - Text Analysis

Appendix Documents

2. Thank You

E-mail user

Aug 18, 2015 18:28:22 Success: Email Sent to: cjroy@vt.edu